Supporting information

1,4-Dihydropyridine-based FA1 site-specific fluorescent probes for the selective detection and quantification of HSA levels in biofluids

S. Shurooque Kanneth,[§] V C Saheer,[#] and Lakshmi Chakkumkumarath[§*]

[§] Department of Chemistry, National Institute of Technology Calicut, Calicut-673601, Kerala, India

[#] Department of Chemistry, Government College Kasaragod, Vidyanagar, Kasaragod-671123, Kerala, India

E-mail: lakshmic@nitc.ac.in

Contents

General information

All the solvents and reagents were purchased from Sigma Aldrich, TCI, Thermofischer, SRL or Spectrochem and used without further purification unless otherwise mentioned. Thin layer chromatography (TLC) was performed on silica gel plates (60 F_{254}, 0.25 mm, Merck) and components were analyzed using UV light or by treating TLC plates with $KMnO_4$ solution or iodine. Chromatographic separation was carried out on 100-200 mesh silica gel. ^{1}H and $^{13}C\{^{1}H\}$ NMR spectra were measured using a 500 MHz JEOL ECZR spectrometer. High-resolution mass spectra (HRMS) were recorded on a Water Q–Tofmicro^{TM} spectrometer with lock spray or Waters Synapt XS high-resolution mass spectrometer. Electronic absorption spectra were recorded using a Shimadzu UV 2600 spectrophotometer and the emission spectra were measured on a Perkin Elmer LS-45 fluorescence spectrometer. The slit-width was adjusted during both excitation and emission measurements using appropriate filters. Fluorescence lifetime data were acquired using Horiba Fluorolog 3 TCSPC system equipped with 290 nm NanoLED light source and analyzed using DAS 6 software.

General analysis methods

Stock solutions of probes (1 mM) and HSA (0.1 mM) were prepared in MeCN and PBS buffer (pH 7.4, 1 mM), respectively. Stock solutions (1 mM) of drugs for displacement studies and interfering species for selectivity studies were prepared either in DMSO or distilled water based on solubility. Detailed methods of analysis are described below.

HSA titration: 1.66 μM solution of the probes was prepared by adding 5 μL of their stock solution into 3 mL of PBS buffer (pH 7.4, 1 mM). Subsequently, HSA solutions were incrementally added, allowed to stand for 1 minute, and recorded the emission spectra.

Limit of detection: The limit of detection (LoD) was calculated using the equation $3\sigma/k$, where σ is the standard deviation of blank measurements and k is the slope of the curve obtained by plotting fluorescence intensity *vs* HSA concentration.

Selectivity studies: To the probe solutions prepared in 3 mL PBS buffer, 1 eq. or 5 eq. of competing species (globulin, lipase, lysozyme, pepsin, trypsin, DTT, GSH, etc.) were added and shaken for 1 minute and recorded the emission spectra.

Job's plot: HSA-probe mixture at different molar ratios was prepared while maintaining total

concentration at 3.33 μM in 3 mL PBS buffer. The stoichiometric point is obtained from the graph of [HSA]/([HSA]+[PROBE]) against fluorescence intensity.

HSA quantification in blood serum: The permission for the experiments with human serum samples was provided by the Institutional Ethical Committee, National Institute of Technology Calicut. Standard serum from a healthy individual ([HSA] = 4.00 g/dL, determined via the BCG technique) was collected from NITC health centre and diluted 10 times using PBS buffer (pH 7.4, 1 mM). The diluted serum (1-20 μL) was added in increments to 3 mL of 1.66 μM probe solution in PBS buffer (pH 7.4, 1 mM). After each addition, the mixture was allowed to stand for 1 minute, and the fluorescence spectrum was recorded. A standard calibration curve was generated by plotting fluorescence intensity against serum concentration. Three serum samples were collected from random people ([HSA] = 3.8 g/dL, 3.9 g/dL, and 4.1 g/dL, respectively based on the BCG test) and two samples were collected from those who were clinically diagnosed with hypoalbuminemia ([HSA] = 2 g/dL and 2.2 g/dL, respectively). Albumin levels in these serum samples were calculated based on the equation $C_{HSA}/C_{STD} = F/F_{STD}$, where C_{HSA} and C_{STD} are the concentrations of HSA in unknown and standard samples, respectively. F and F_{STD} are the corresponding fluorescence intensities on addition of a particular volume of serum from the unknown and standard samples.

HSA quantification in urine: The permission for the experiments with human urine samples was provided by the Institutional Ethical Committee, National Institute of Technology Calicut. Urine sample was collected from a healthy donor (confirmed to be devoid of HSA through clinical testing). The collected sample was spiked with 3.33 μM (213 mg/L) of HSA. The fluorescence responses were then measured by adding 0-300 μL of this urine to the probe in 3 mL PBS buffer (pH 7.4, 1 mM). A standard calibration curve was generated by plotting fluorescence intensity against serum concentration. Volumes of 70 μL, 140 μL, and 210 μL of the HSA spiked urine sample were then added to the probe solution in 3 mL of PBS buffer. The emission intensity at 515 nm was measured, and the concentration of HSA was obtained from the calibration plot.

Displacement studies: 1:1 probe-HSA solutions (1.66 μM) were prepared in 3 mL PBS buffer. 1 eq., 2 eq., 3 eq., 4 eq., 5 eq., and 10 eq. of the drugs (ibuprofen, flurbiprofen, warfarin, salicylic acid, and hemin) were added to the above solution and mixed well. This solution was allowed to stand for 2 minutes before recording the emission spectra. The inhibition percentage at each addition was calculated using the equation, inhibition (100%) = $(F_{[HSA\text{-}PROBE]}\text{-}F)/ F_{[HSA\text{-}}$

$_{PROBE}$-$F_{[PROBE]}$), where F, is fluorescence intensity in the presence of inhibitor drug, $F_{[HSA-PROBE]}$ and $F_{[PROBE]}$ are fluorescence intensity of probe-HSA complex and free probe respectively.

Molecular docking studies: To set up the molecular docking studies with the DHP derivatives, we first prepared its initial 2D structures in ChemDraw 12 software and the saved 2D structures were subsequently converted to 3D structure (mol2 format) in Chem3D software. The structures thus obtained were cleaned and a geometry optimization was carried out on each molecule in a general AMBER force field (GAFF) environment in Avogadro software. A further refinement of geometry was carried out using the semi-empirical PM6 level of theory implemented in Gaussian 16 software and the resulting geometry was saved in a pbd format. Discovery Studio visualizer software was then used to retrieve the coordinates of the receptor (human serum albumin, PDB ID: 1N5U) from the protein databank and extracting the native heme ligand. Both receptor and native ligand coordinates were saved separately in the pdb format.

3D coordinates of atoms, their partial charges, and information about atom types of the receptor and ligand information necessary for docking were then prepared in AutoDockTools (ADT version 1.5.6) software of Scripps Research Institute. The receptor protein file was prepared after merging the nonpolar hydrogens, assigning Kollman charges, and saving the file in pdbqt format. The pdbqt file for the ligand molecules was also prepared similarly. These pdbqt files were then used to prepare grid and docking parameter files required to run autogrid and autodock executables for docking studies. The docking calculations were then initiated using a prewritten bash script in CYGWIN runtime environment under Windows OS. The script file can also be downloaded directly from the link: https://bit.ly/3v6dnkZ . The results were analysed in AutoDock Tools and Discovery Studio Visualizer software.

Experimental procedure

Synthesis and characterisation

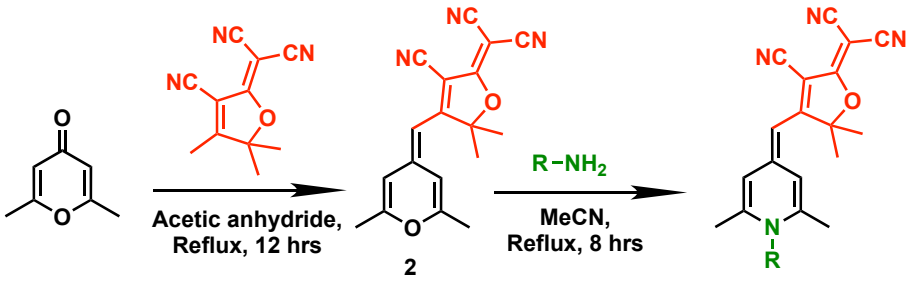

Scheme S1. Synthesis of **DHP-DCDHF** derivatives.

Preparation of DHP-DCDHF derivatives: A mixture of **2** (2.9 mmol) and the corresponding amine (10 mmol) in 10 mL of acetonitrile was heated under reflux conditions for 36 hrs. After the mixture was cooled to room temperature, the solvent was removed using a rotary evaporator, and the residue was poured into ethyl acetate. The precipitate obtained was filtered, washed with ethyl acetate, and dried to yield the pure compound. Due to the limited solubility in most of the solvents, we could not record the ^{1}H NMR spectrum of **2h** and **2i** and ^{13}C NMR spectra of **R-2b**, **S-2b**, **2h**, **2i**, and **2j**.

R-2b: Yield = 32%. ^{1}H-NMR (25^{0}C, 500 MHz, $CDCl_3$) δ 7.44 -7.39 (m, 3H), 7.09 (d, *J* = 7.1 Hz, 2H), 6.07 (q, *J* = 6.7 Hz, 1H), 5.14 (s, 1H), 2.04 (d, *J* = 7.2 Hz, 3H), 1.51 (s, 6H). ^{1}H-NMR (-50^{0}C, 500 MHz, $CDCl_3$) δ 7.45 (m, 3H), 7.25 (s, 1H), 7.11 (d, J = 7.2 Hz, 2H), 7.03 (s, 1H), 6.13-6.10 (m, 1H), 5.21 (s, 1H), 2.84 (s, 3H), 2.20 (s, 3H), 2.08 (d, J = 7.1 Hz, 3H), 1.52 (s, 6H). HRMS (ESI) exact mass calcd. for $C_{26}H_{24}N_4NaO$ 431.1848; found $[M+Na]^+$ 431.1846.

S-2b: Yield = 27%. ^{1}H-NMR (500 MHz, $CDCl_3$) δ 7.44-7.37 (m, 3H), 7.09 (d, *J* = 7.2 Hz, 2H), 6.06 (m, 1H), 5.14 (s, 1H), 2.04 (d, *J* = 7.1 Hz, 3H), 1.51 (s, 6H). HRMS (ESI) exact mass calcd. for $C_{26}H_{24}N_4NaO$ 431.1848; found $[M+Na]^+$ 431.1846.

In the ^{1}H NMR spectrum of compounds **R-2b**, **S-2b**, and the racemic mixture **2b**, the C-2 & C-6 methyl groups and C-3 & C-5 hydrogens of the DHP ring were absent when the spectra were recorded at room temperature. The rotameric behaviour of **2b** has already been reported.[1] In the NMR spectra of **R-2b** recorded at -50^{0}C, these peaks were present confirming the rotameric behaviour.

2h: Yield = 17%. HRMS (ESI) exact mass calcd. for $C_{25}H_{24}N_5O$ 410.1981; found $[M+H]^+$ 410.1995.

2i: Yield = 25%. HRMS (ESI) exact mass calcd. for $C_{25}H_{23}N_4O_2$ 411.1821; found $[M+H]^+$ 411.1816.

2j: Yield = 65%. ^{1}H-NMR (500 MHz, $CDCl_3$) δ 7.05 (d, *J* = 20.6 Hz, 2H), 5.09 (s, 1H), 4.49-4.44 (m, 1H), 2.77 (s, 3H), 2.65 (s, 3H), 2.20-2.12 (m, 2H), 2.00 (t, *J* = 15.3 Hz, 4H), 1.47 (s, 6H), 1.45-1.38 (m, 2H), 1.29-1.20 (m, 2H). HRMS (ESI) exact mass calcd. for $C_{24}H_{27}N_4O$ 387.2185; found $[M+H]^+$ 387.2187.

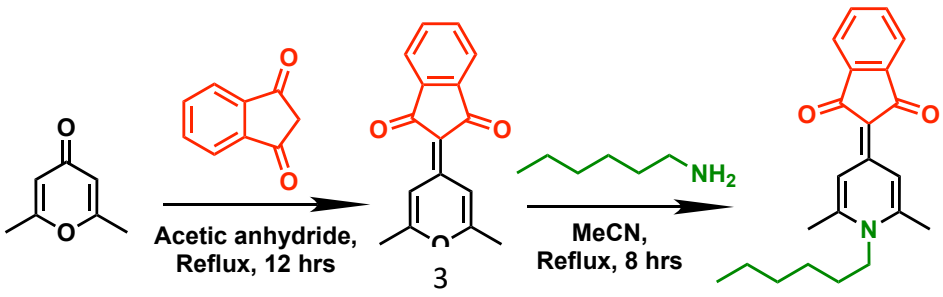

Scheme S2. Synthesis of compound **3d**.

Synthesis of DHP-IND derivatives (3d)

A mixture of the **3** (3 mmol) and the corresponding amine (10 mmol) in 10 mL of acetonitrile was heated under reflux conditions for 12 hrs. After cooling the reaction mixture to room temperature, the solvent was removed using a rotary evaporator under vacuum. The residue thus obtained was triturated with ethyl acetate, the precipitate obtained was filtered and washed with ethyl acetate.

3d: Yield = 57%. ^{1}H-NMR (500 MHz, $CDCl_3$) δ 8.58 (d, J = 9.2 Hz, 2H), 7.60 (m, 2H), 7.46 (m, 2H), 3.84 (brs, 2H), 2.50 (s, 6H), 1.63 (brs, 3H), 1.29 (brs, 6H), 0.87 (t, J = 6.5 Hz, 3H). ^{13}C{^{1}H}-NMR (125 MHz, $CDCl_3$) δ 192.9, 149.8, 149.7, 148.3, 140.3, 131.8, 120.0, 117.1, 49.5, 31.1, 29.6, 26.4, 22.5, 20.8, 13.9. HRMS (ESI) exact mass calcd. for $C_{22}H_{26}NO_2$ 336.1964; found $[M+H]^+$ 336.1972.

NMR and HRMS Spectra

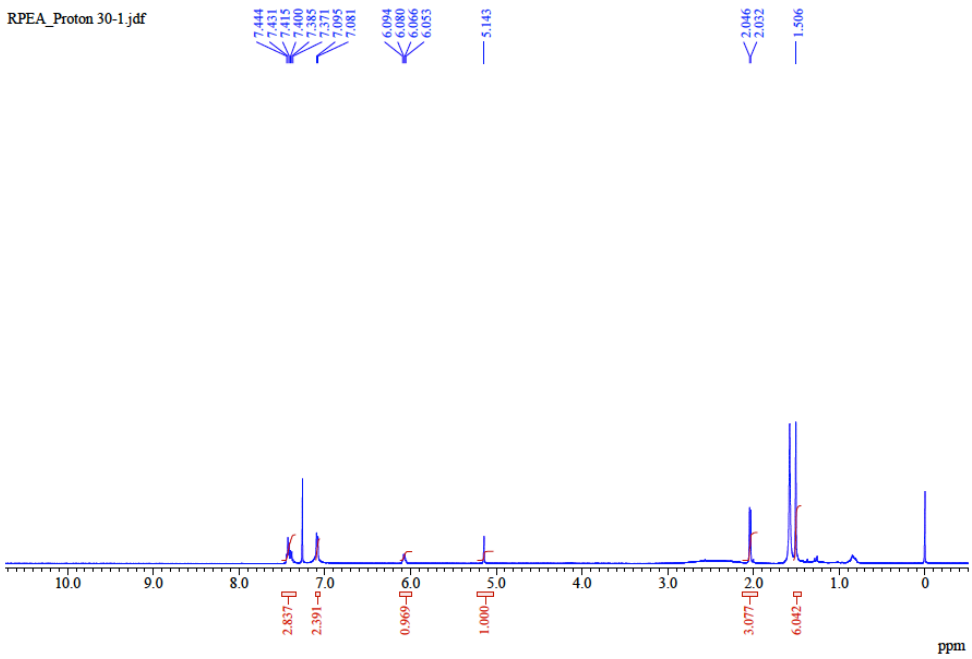

Spectra S1. ^{1}H-NMR spectra of **R-2b** (25°C, 500 MHz, $CDCl_3$).

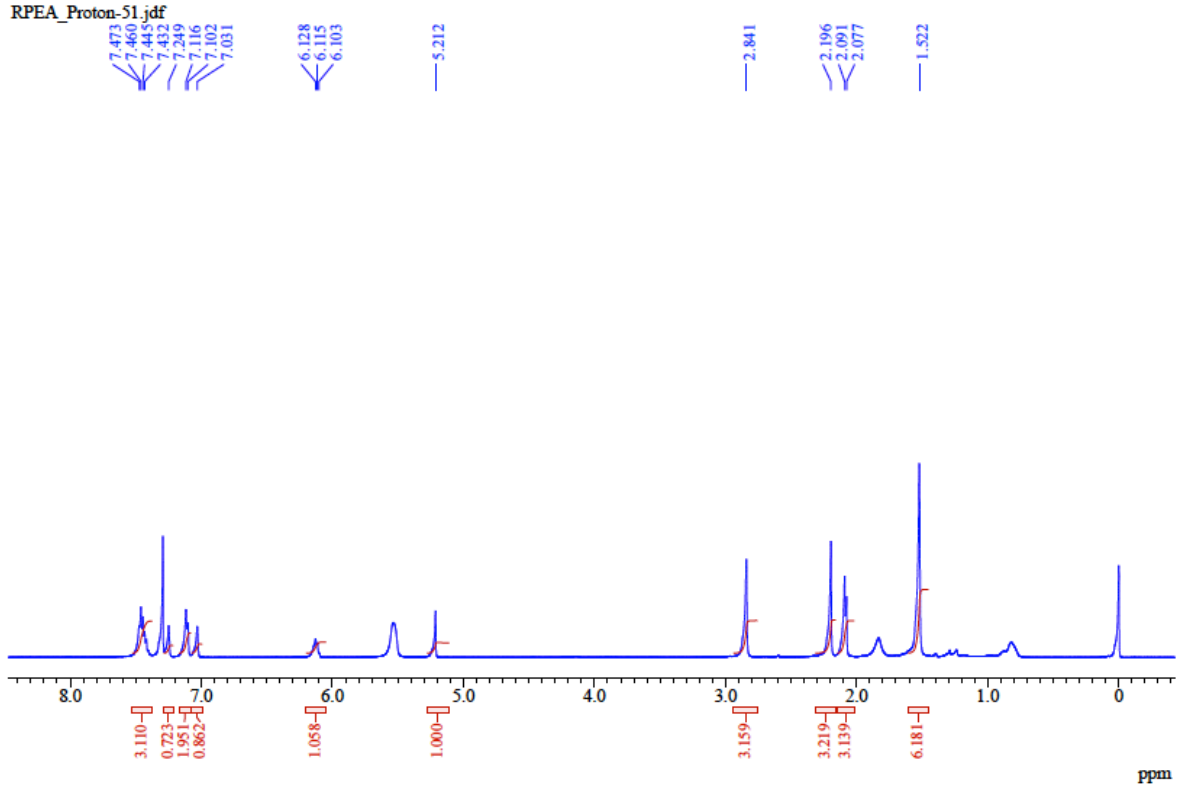

Spectra S2. ^{1}H-NMR spectra of **R-2b** (-50°C, 500 MHz, $CDCl_3$).

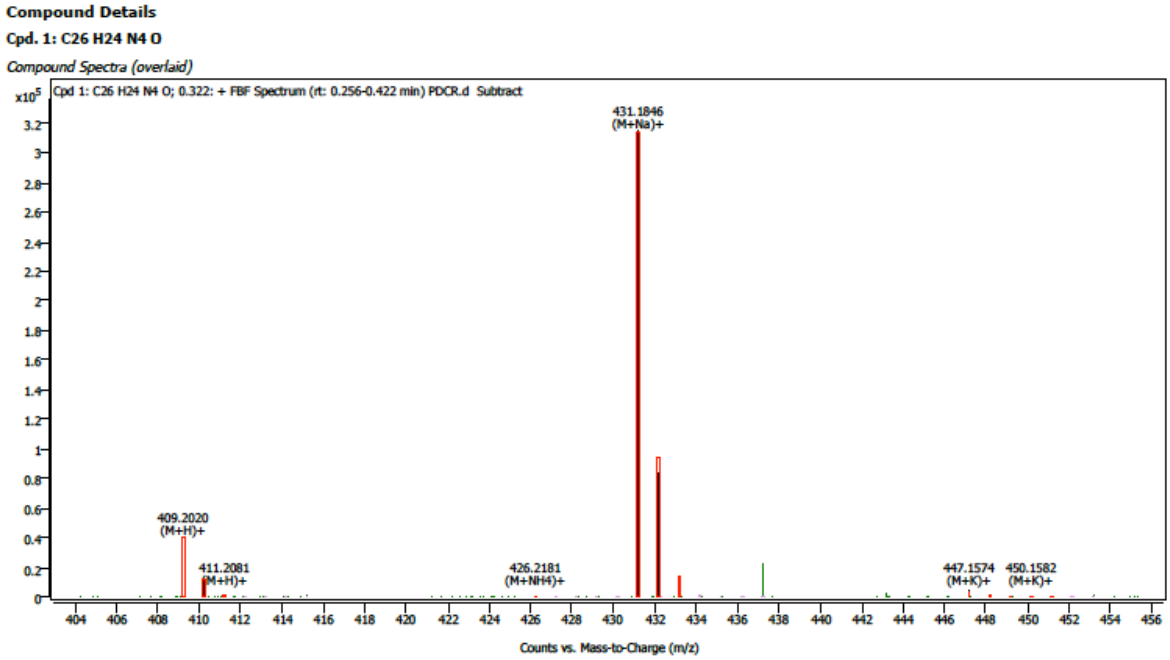

Compound ID Table

Cpd	Formula	Mass (Tgt)	Calc. Mass	Mass	Species	Diff(Tgt.ppm)	mDa
1	C26 H24 N4 O	408.1950	408.1952	409.2020 426.2181 431.1846 447.1574	(M+H)+ (M+NH4)+ (M+Na)+ (M+K)+	0.37	0.15

Spectra S3. HRMS of **R-2b**.

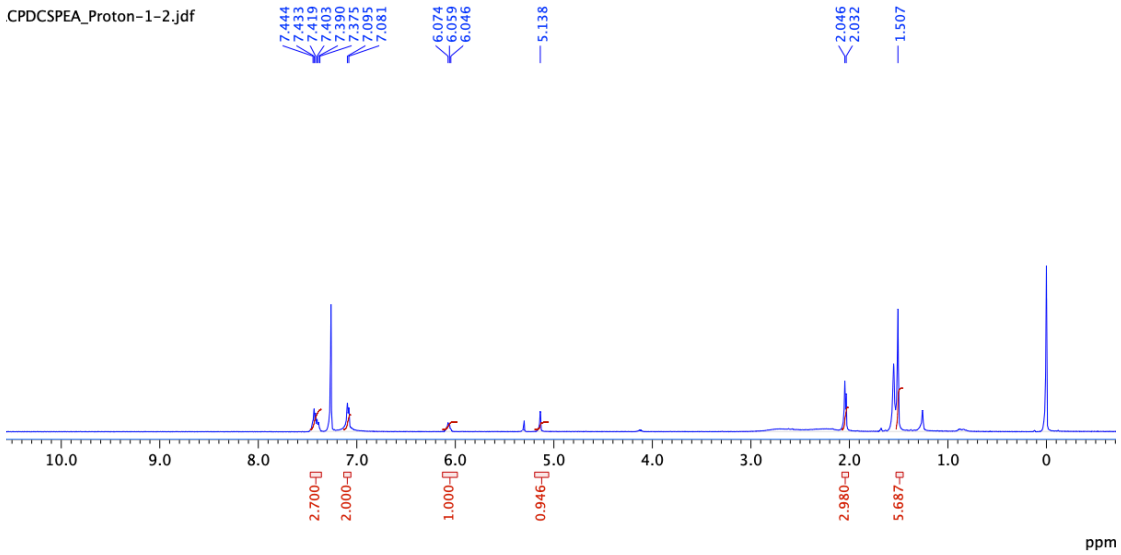

Spectra S4. ^{1}H-NMR spectra of **S-2b** (500 MHz, $CDCl_3$).

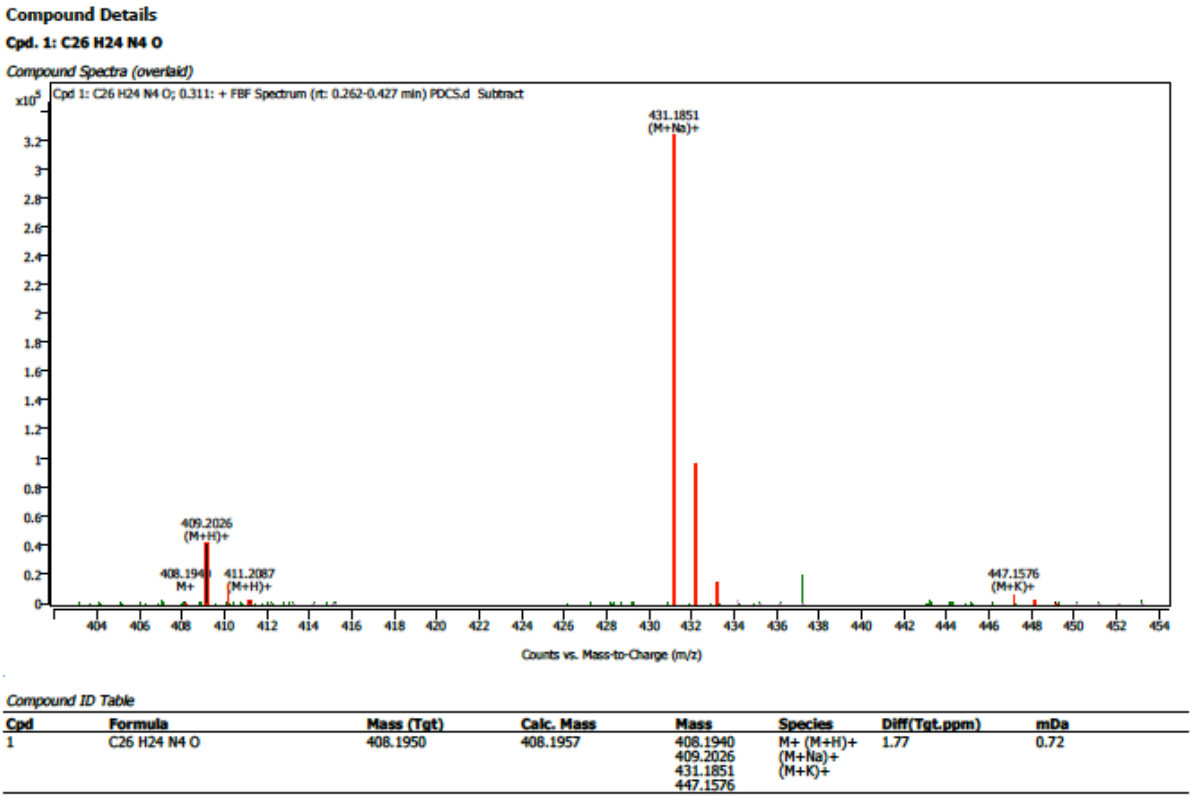

Spectra S5. HRMS of **S-2b**.

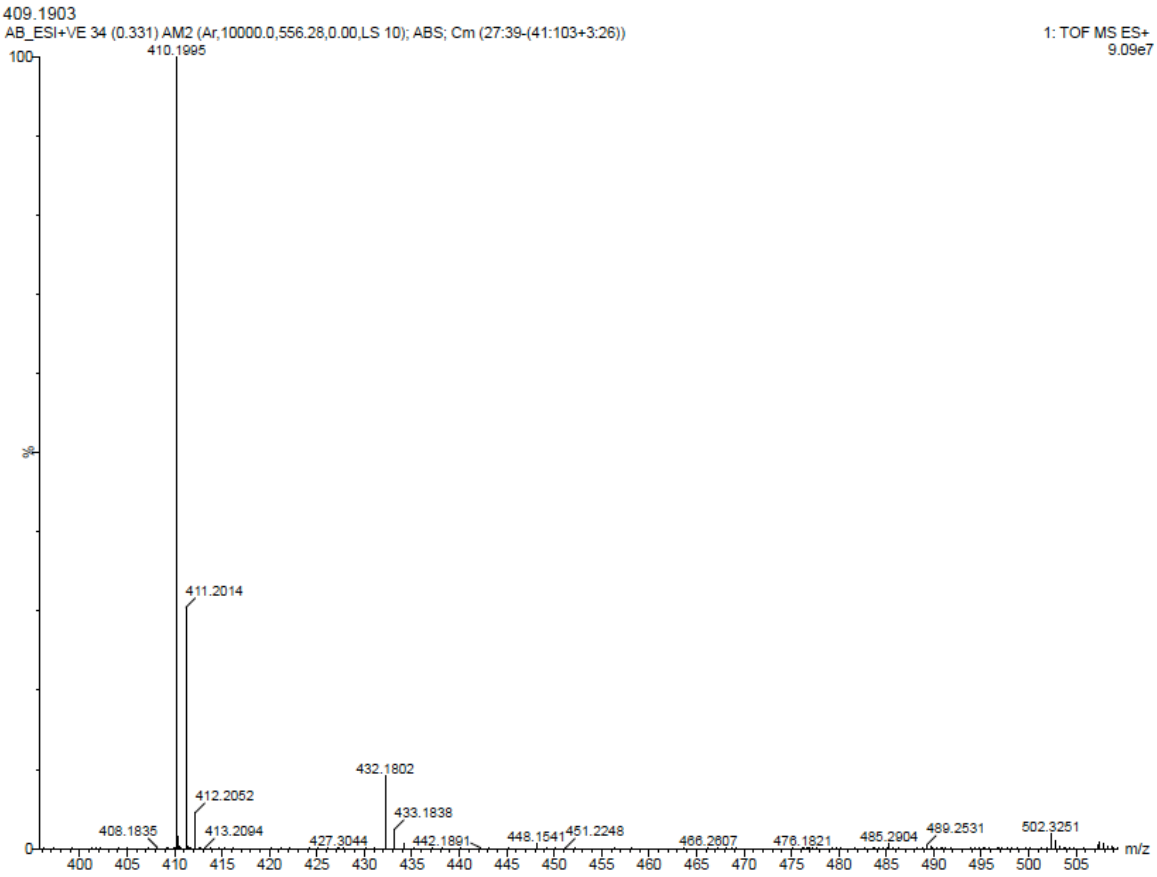

Spectra S6. HRMS of **2h**.

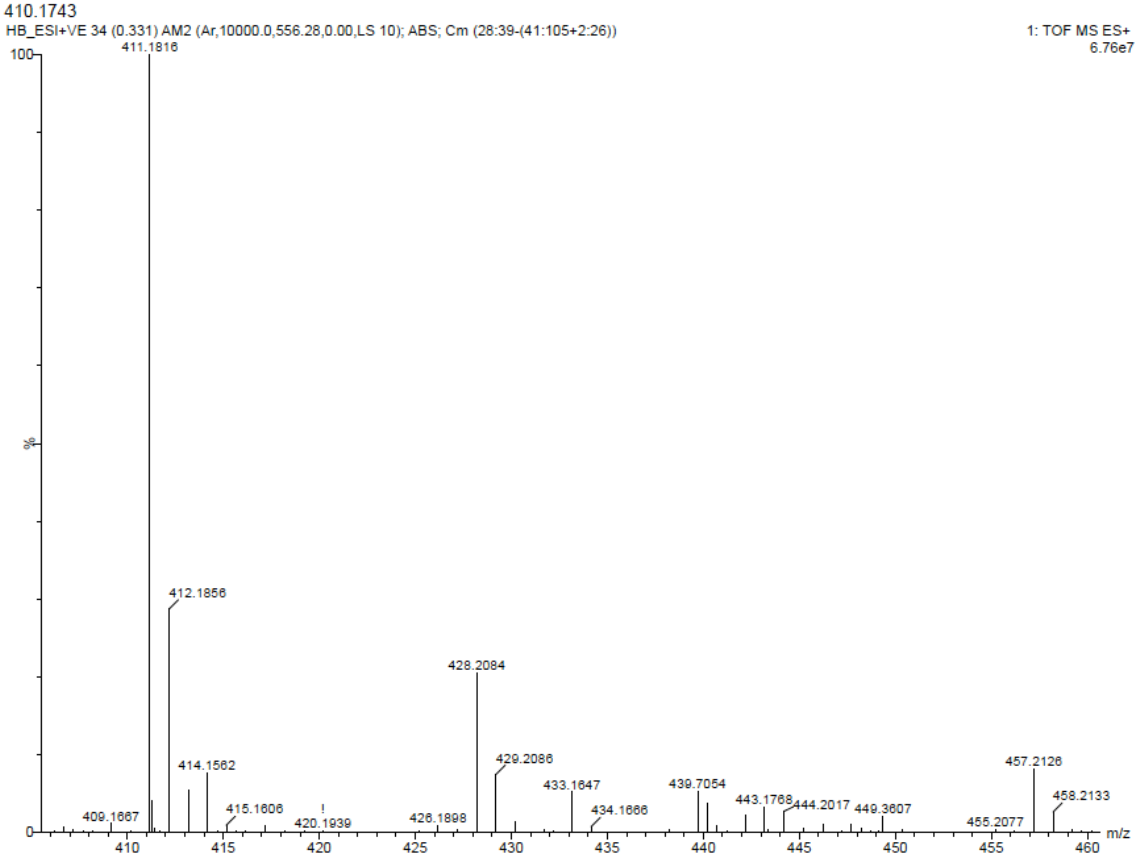

Spectra S7. HRMS of **2i**.

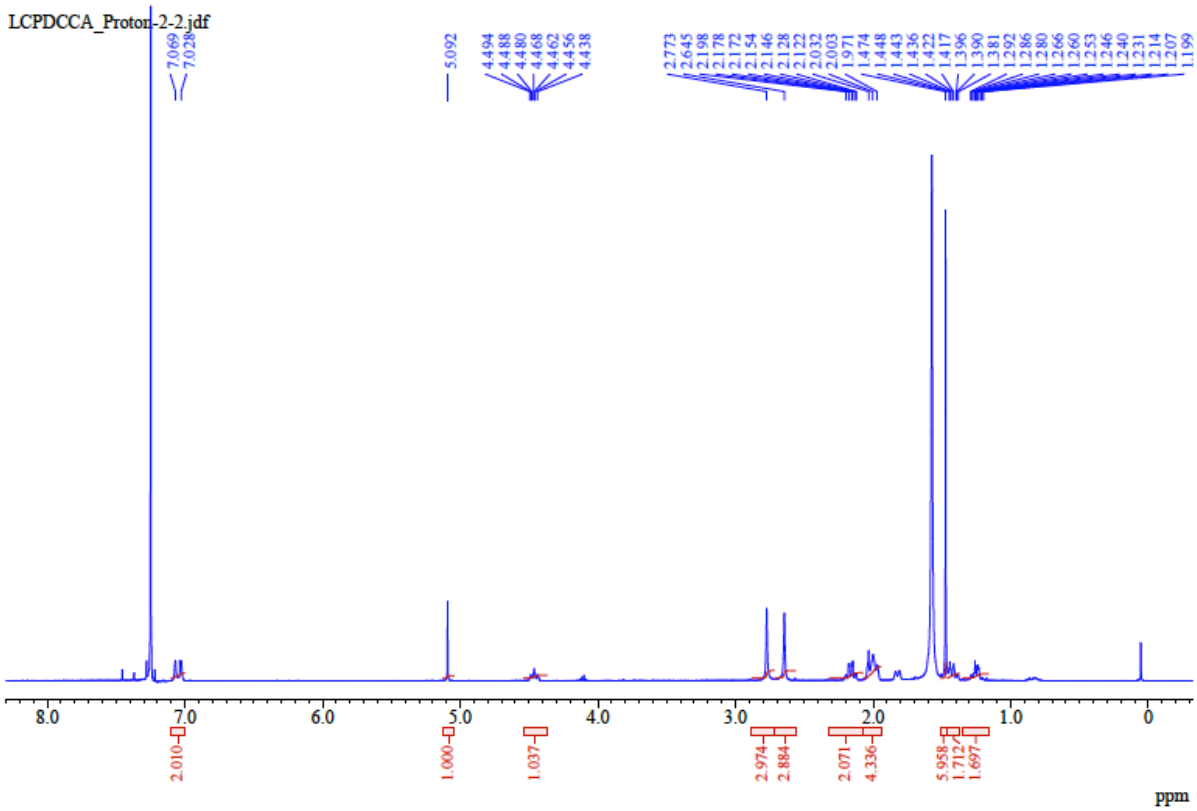

Spectra S8. ^{1}H-NMR spectra of **2j** (500 MHz, $CDCl_3$).

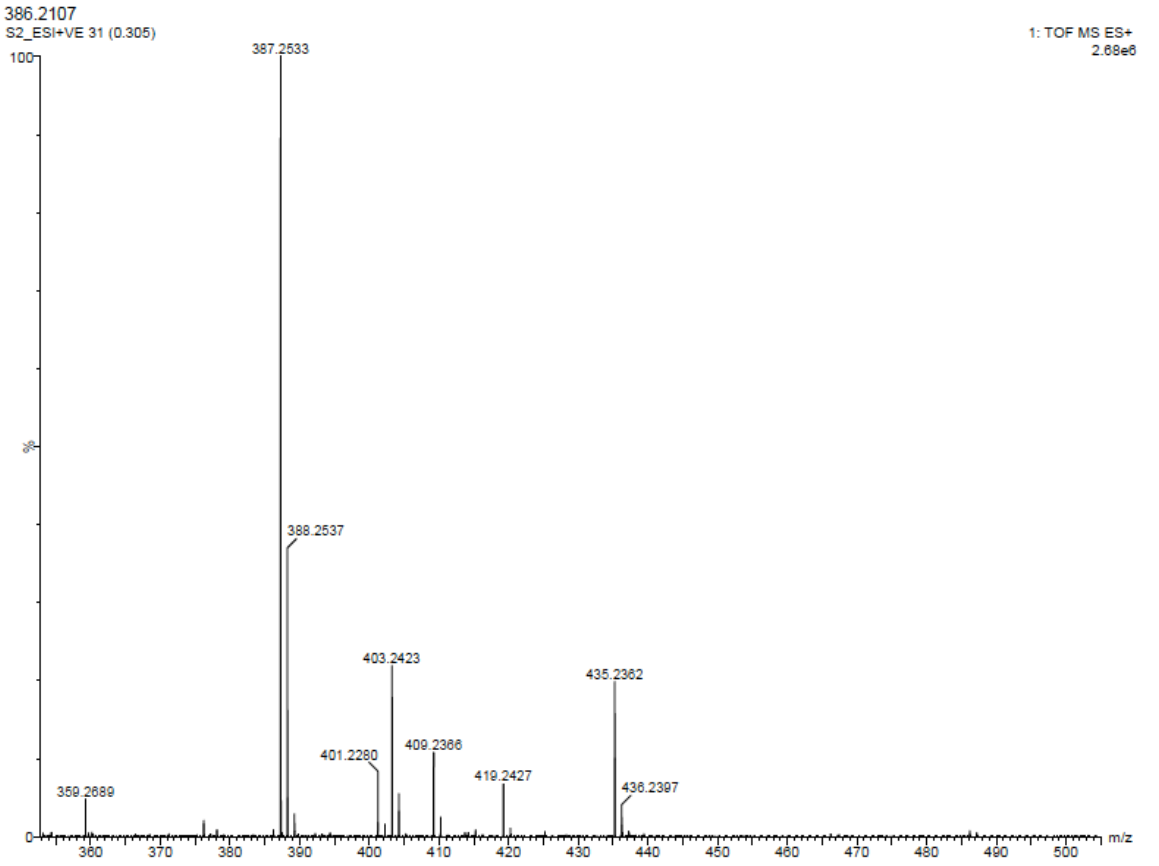

Spectra S9. HRMS of **2j**.

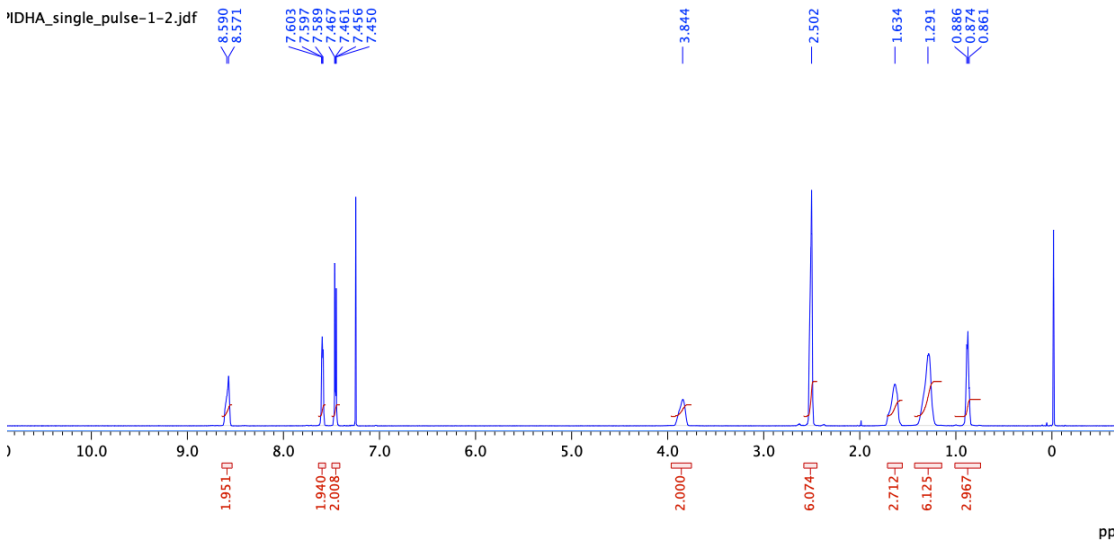

Spectra S10. ^{1}H-NMR spectra of **3d** (500 MHz, $CDCl_3$).

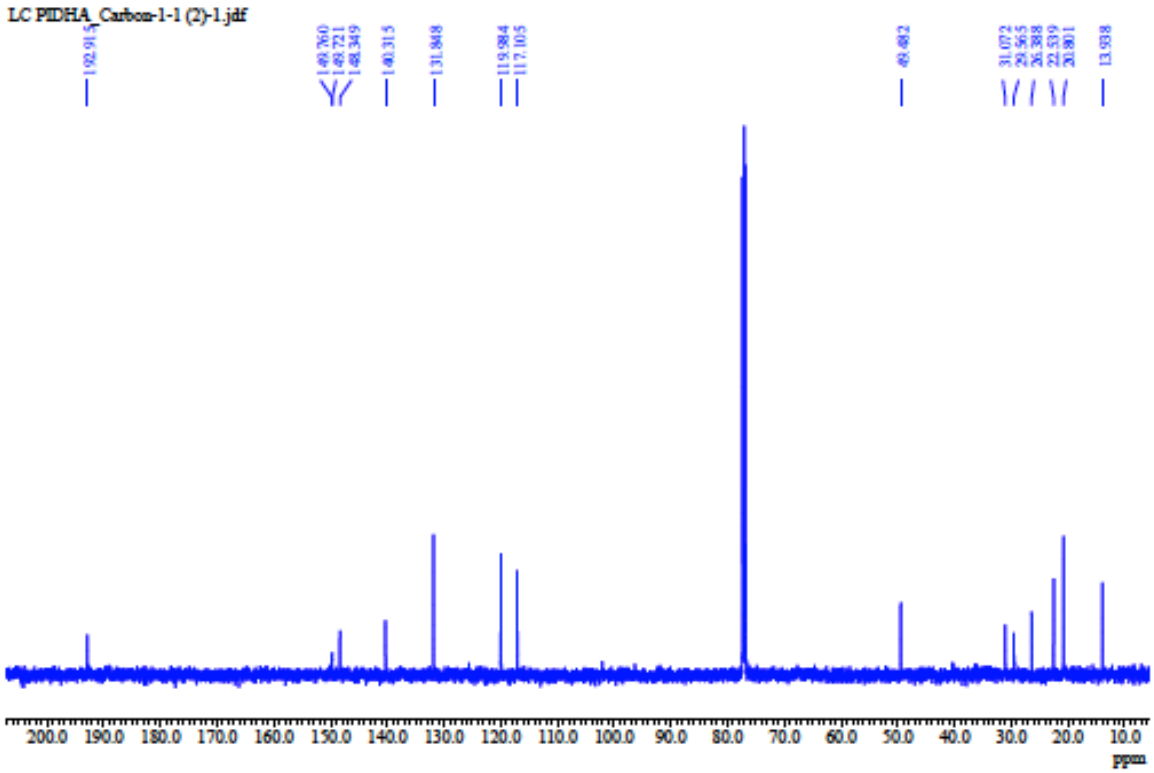

Spectra S11. ^{13}C{^{1}H}-NMR spectra of **3d** (125 MHz, $CDCl_3$).

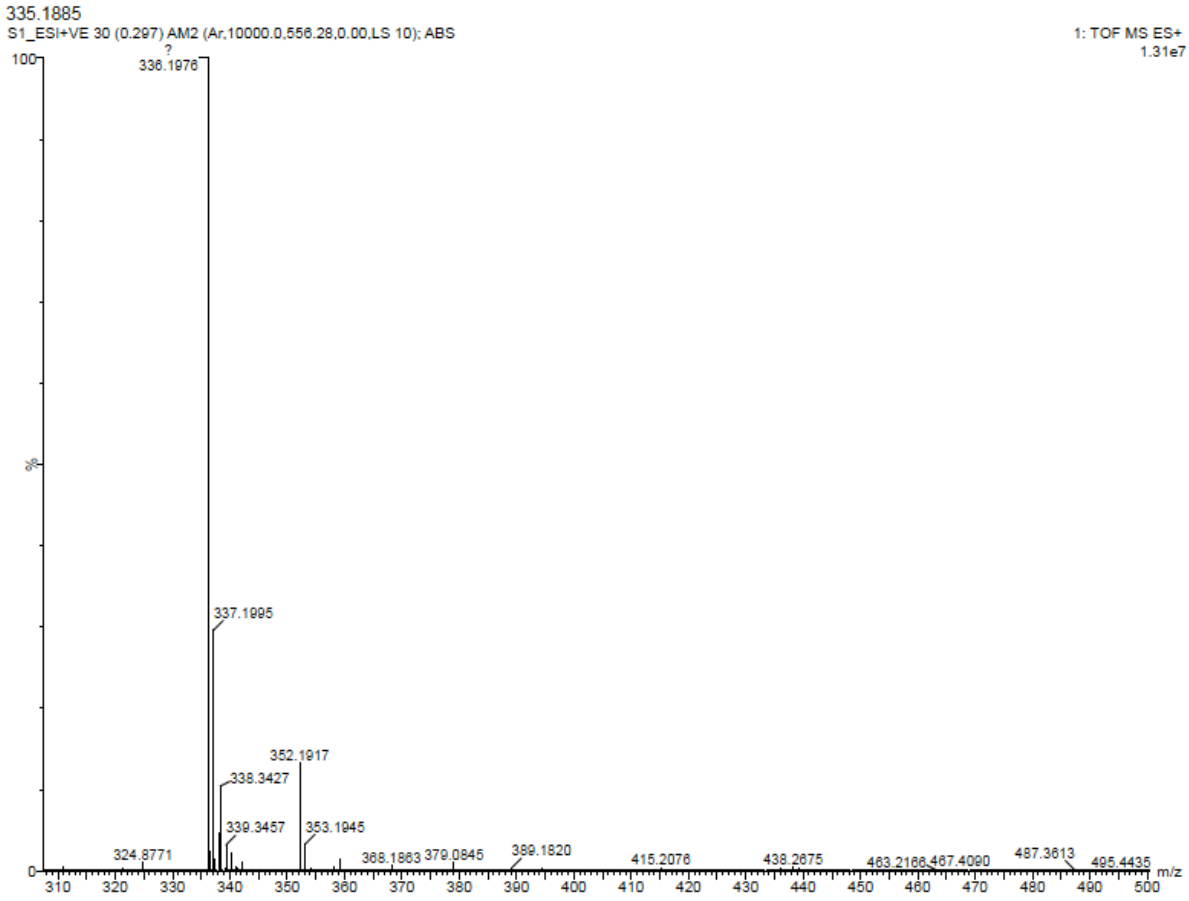

Spectra S12. HRMS of **3d**.

Solvatochromism

Table S1. Absorption and emission maxima of compounds in different solvents.

		R-2b	S-2b	2h	2i	2j
Toluene	$\lambda_{ab.max}$	525	524	517	517	521
	$\lambda_{ems.max}$	558	558	566	533	545
Chloroform	$\lambda_{ab.max}$	506	506	508	500	501
	$\lambda_{ems.max}$	539	540	535	529	533
MeCN	$\lambda_{ab.max}$	488	489	485	484	482
	$\lambda_{ems.max}$	524	524	519	522	524
DMSO	$\lambda_{ab.max}$	487	487	485	484	482
	$\lambda_{ems.max}$	524	524	519	519	520

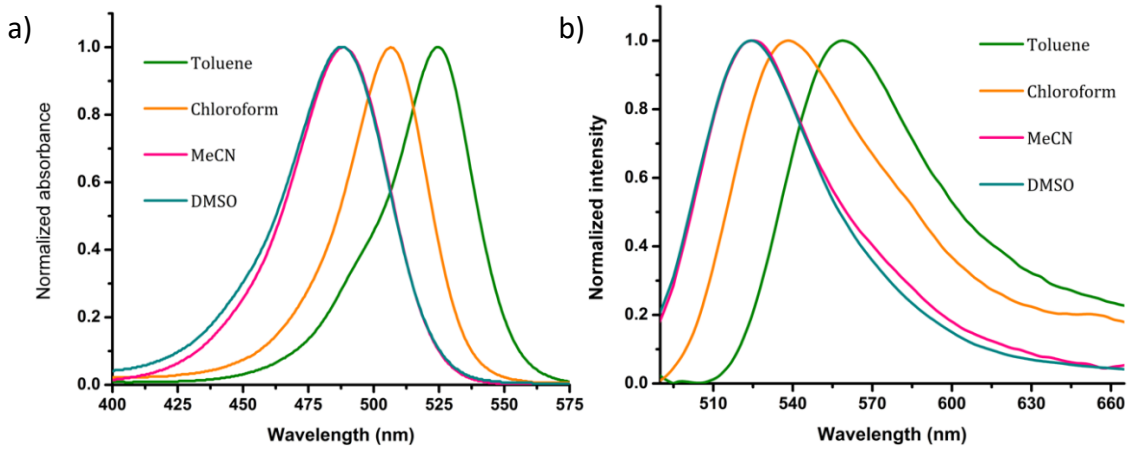

Figure S1. Normalized a) absorption and b) emission spectra of 3.33 x 10^{-5} M solution of **R-2b** in different solvents (λ_{ex} = 470 nm).

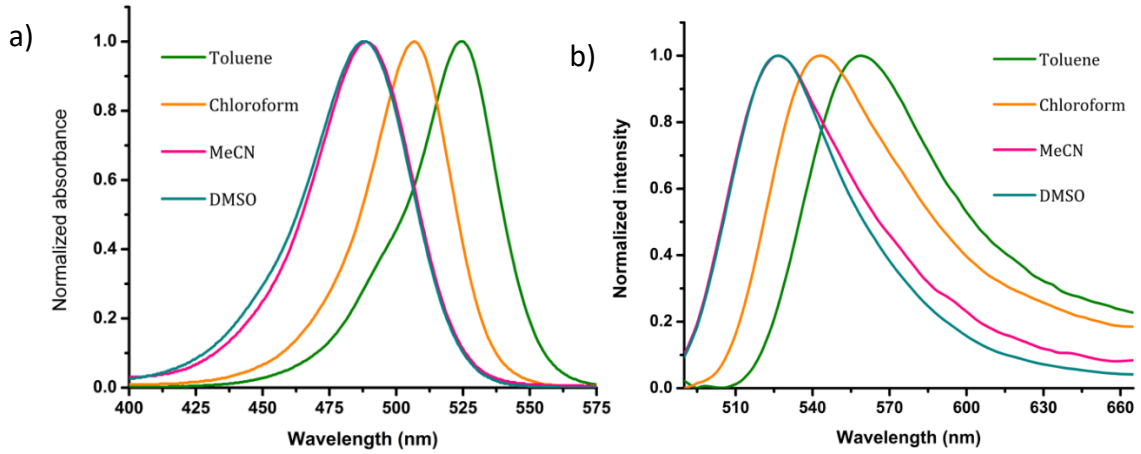

Figure S2. Normalized a) absorption and b) emission spectra of 3.33 x 10^{-5} M solution of **S-2b** in different solvents (λ_{ex} = 470 nm).

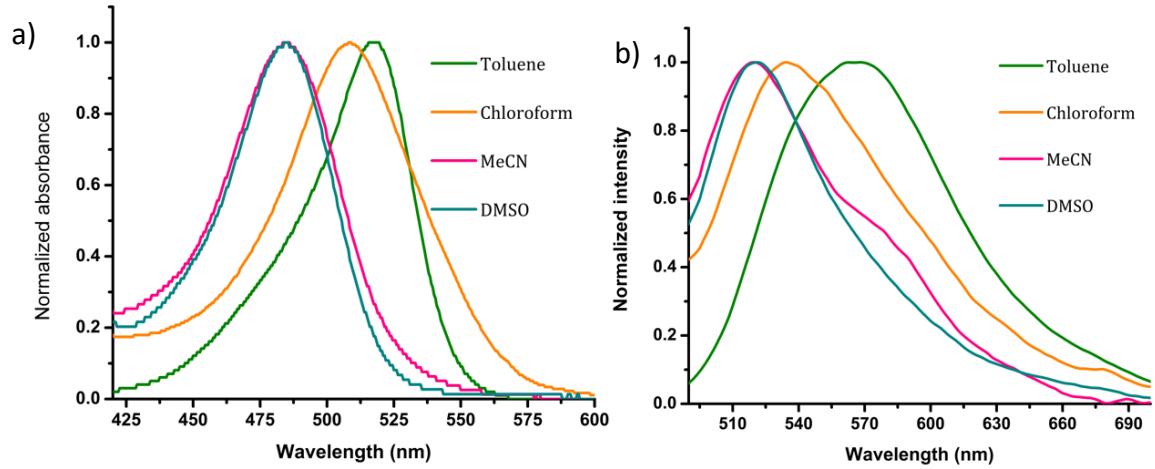

Figure S3. Normalized a) absorption and b) emission spectra of 3.33 x 10^{-5} M solution of **2h** in different solvents (λ_{ex} = 470 nm).

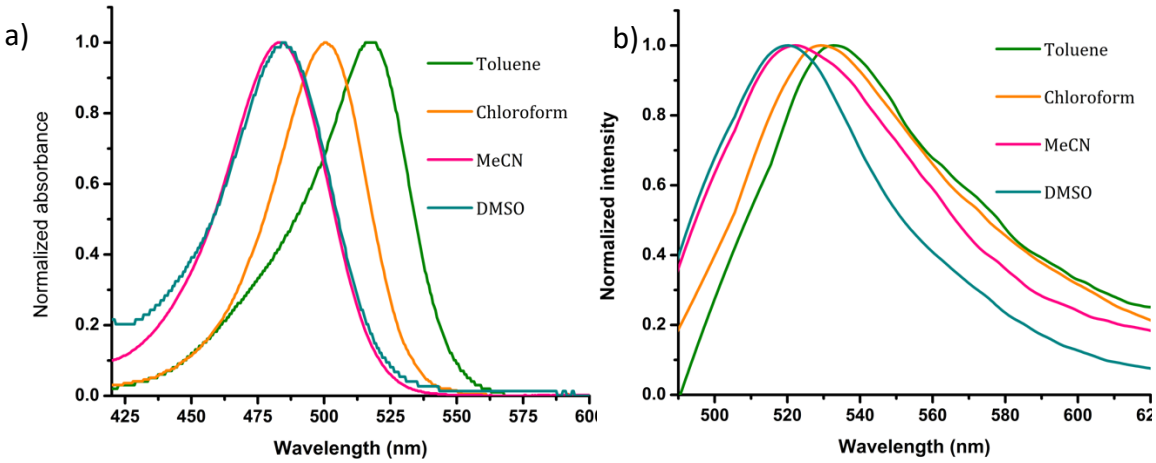

Figure S4. Normalized a) absorption and b) emission spectra of 3.33 x 10^{-5} M solution of **2i** in different solvents (λ_{ex} = 470 nm).

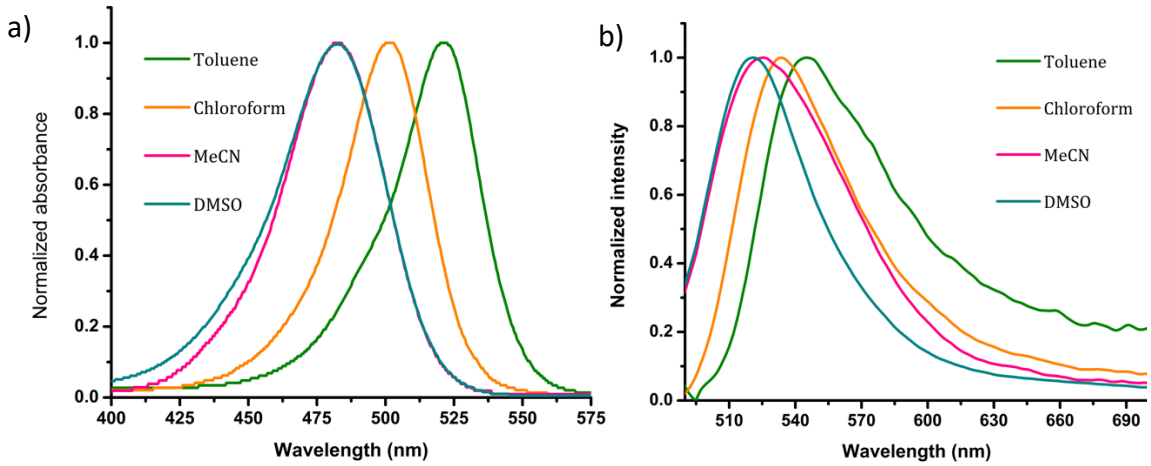

Figure S5. Normalized a) absorption and b) emission spectra of 3.33 x 10^{-5} M solution of **2j** in different solvents (λ_{ex} = 470 nm).

Viscosity-dependant emission

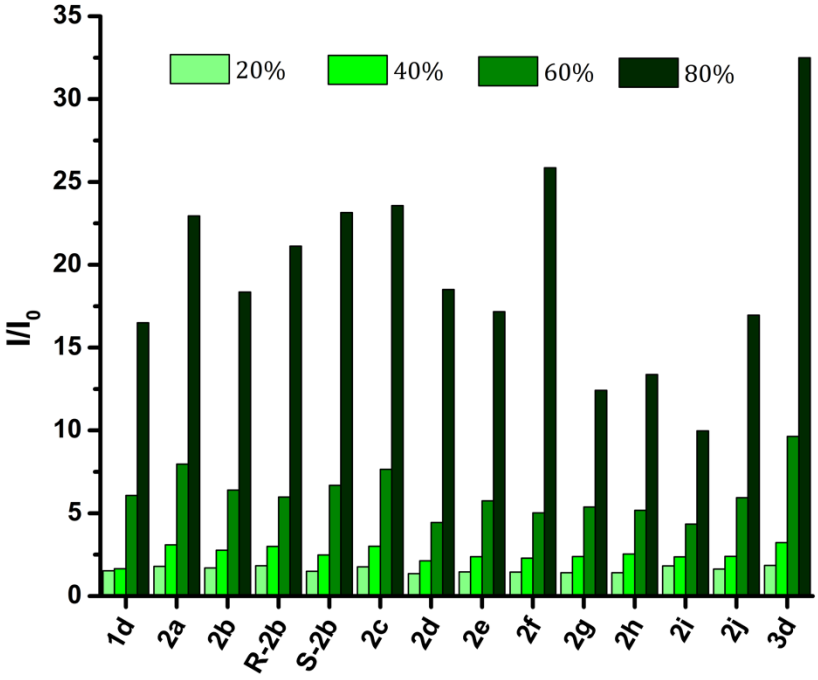

Figure S6. Emission intensity of 16.66 μM solutions of compounds in methanol with increasing percentages of glycerol. The percentages mentioned in the figure correspond to that of glycerol.

HSA Sensing

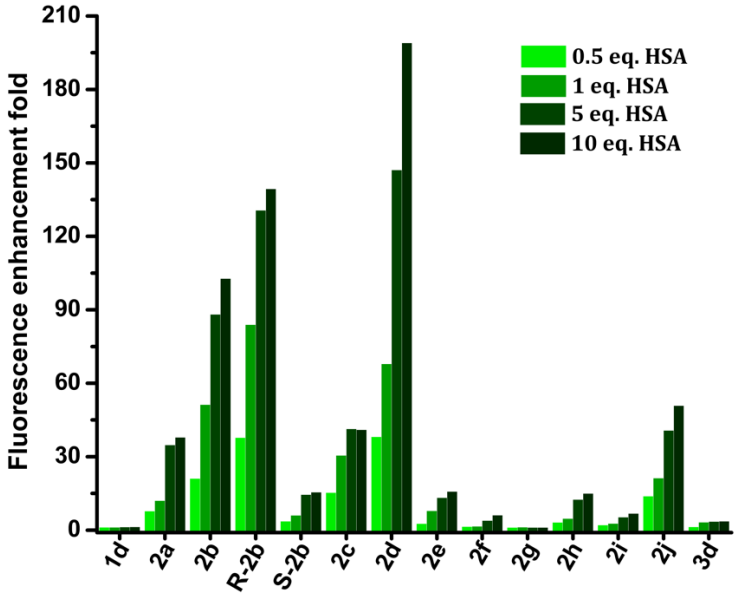

Figure S7. Comparison of fluorescence enhancement of **1d**, **2a-j**, and **3d** in the presence of 0.5, 1, 5, and 10 eq. of HSA in PBS buffer (1 mM, pH=7.4).

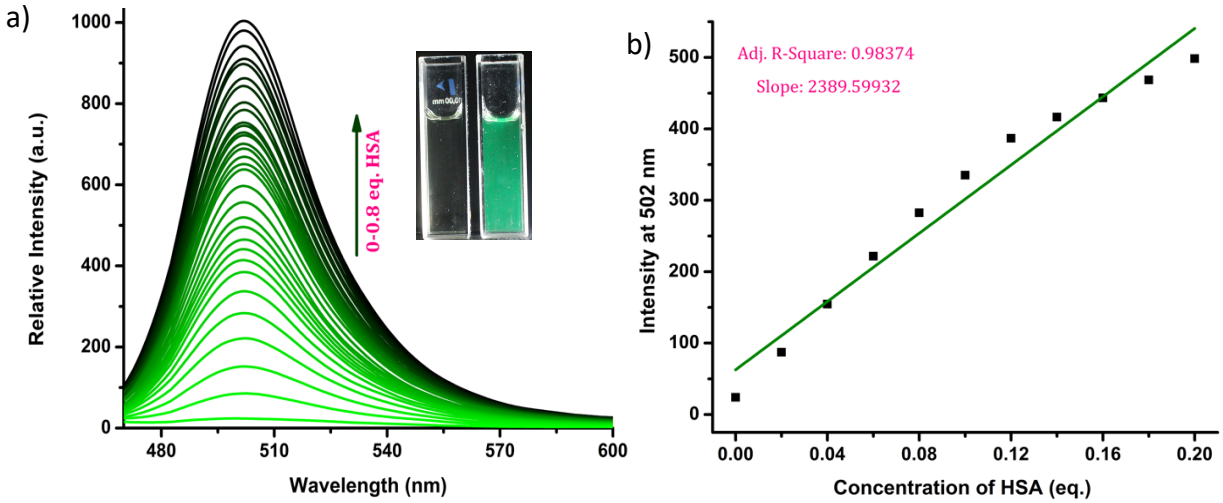

Figure S8. a) Fluorescence spectra of **2d** (1.66 µM) on incremental addition of HSA (0-0.8 eq.) in PBS buffer (pH 7.4, 1 mM) and photograph of **2d** in the absence and presence of HSA under flashlight (inset). b) Linear relationship between the concentration of HSA and fluorescence intensity of **2d** at 502 nm (λ_{ex}= 460 nm).

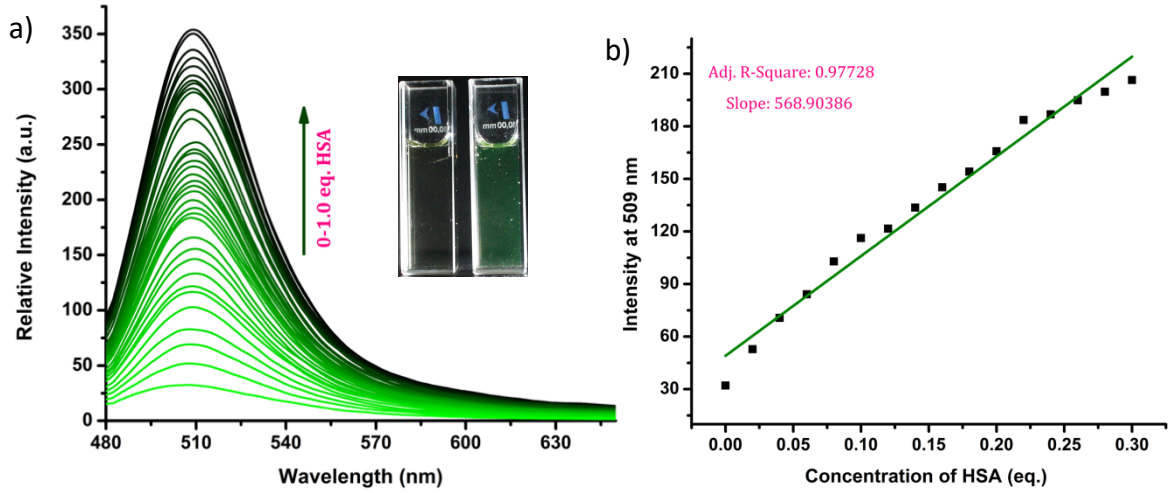

Figure S9. Fluorescence spectra of **2a** (1.66 µM) on incremental addition of HSA (0-1 eq.) in PBS buffer (pH 7.4, 1 mM) and photograph of **2a** in the absence and presence of HSA under flashlight (inset). b) Linear relationship between the concentration of HSA and fluorescence intensity of **2a** at 509 nm (λ_{ex}= 460 nm).

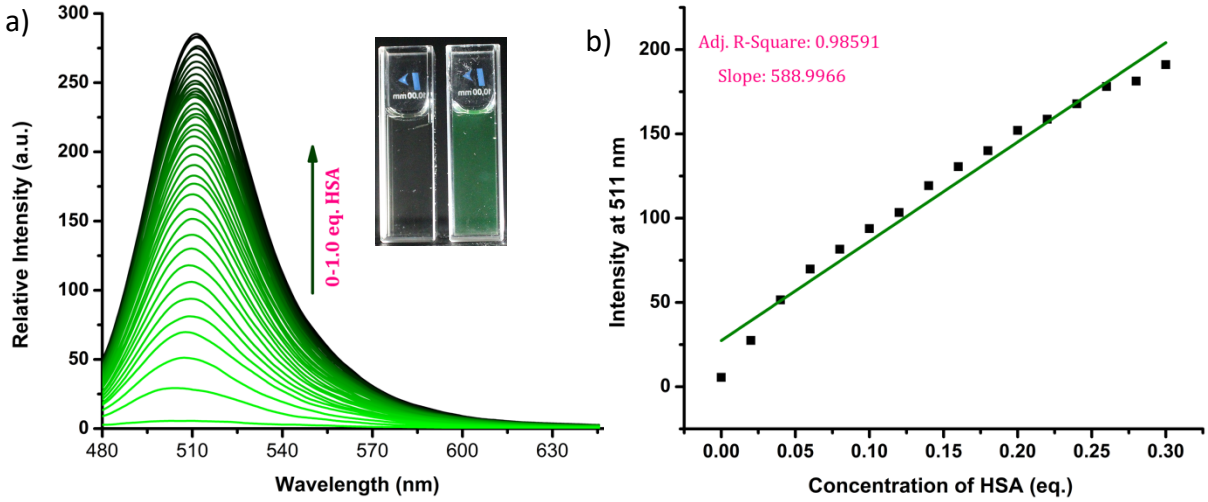

Figure S10. Fluorescence spectra of **2b** (1.66 µM) on incremental addition of HSA (0-1 eq.) in PBS buffer (pH 7.4, 1 mM) and photograph of **2b** in the absence and presence of HSA under flashlight (inset). b) Linear relationship between the concentration of HSA and fluorescence intensity of **2b** at 511 nm (λ_{ex}= 460 nm).

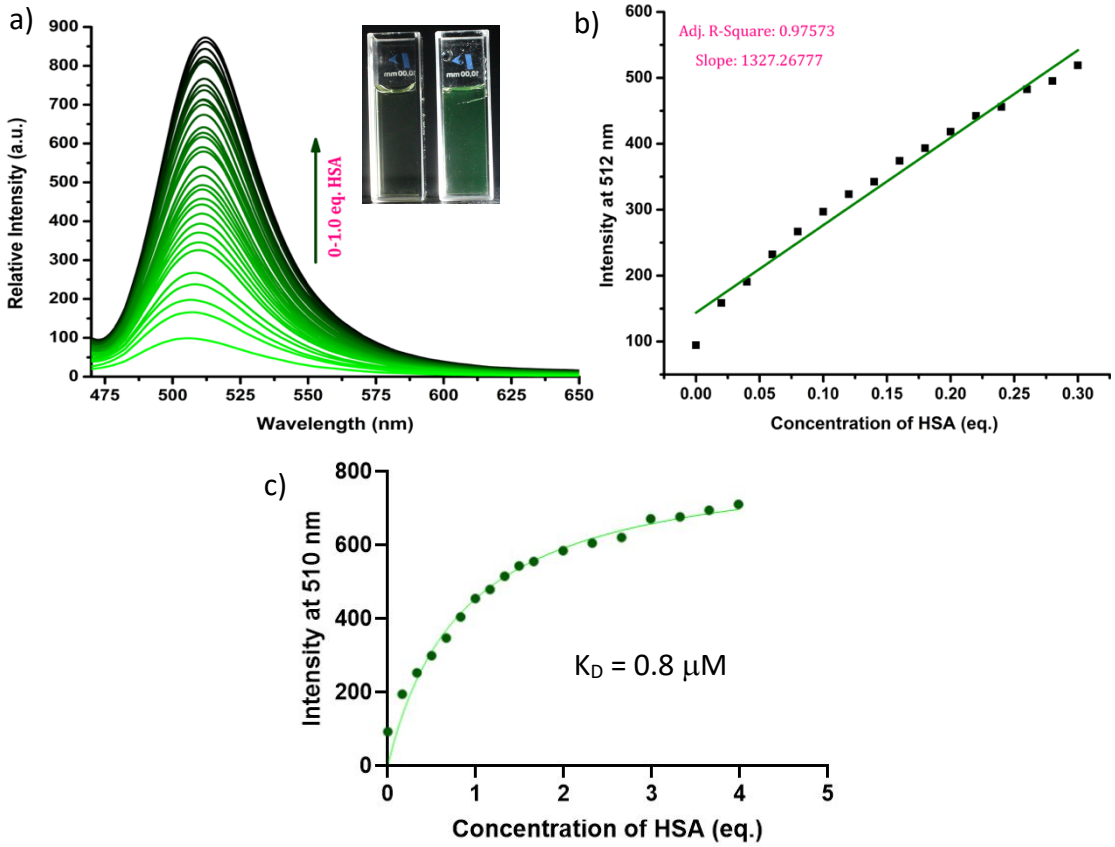

Figure S11. Fluorescence spectra of **S-2b** (1.66 µM) on incremental addition of HSA (0-1 eq.) in PBS buffer (pH 7.4, 1 mM) and photograph of **S-2b** in the absence and presence of HSA under flashlight (inset). b) Linear relationship between the concentration of HSA and fluorescence intensity of **S-2b** at 512 nm (λ_{ex}= 460 nm). c) Binding curve of **S-2b** with HSA.

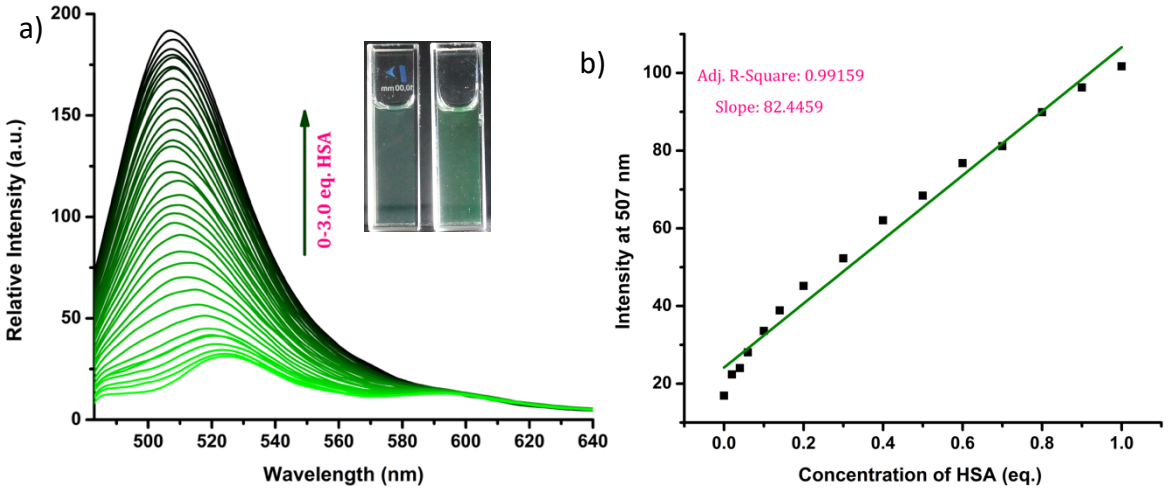

Figure S12. a) Fluorescence spectra of **2e** (1.66 μM) on incremental addition of HSA (0-3 eq.) in PBS buffer (pH 7.4, 1 mM) and photograph of **2e** in the absence and presence of HSA under flashlight (inset). b) Linear relationship between the concentration of HSA and fluorescence intensity of **2e** at 507 nm (λ_{ex}= 460 nm).

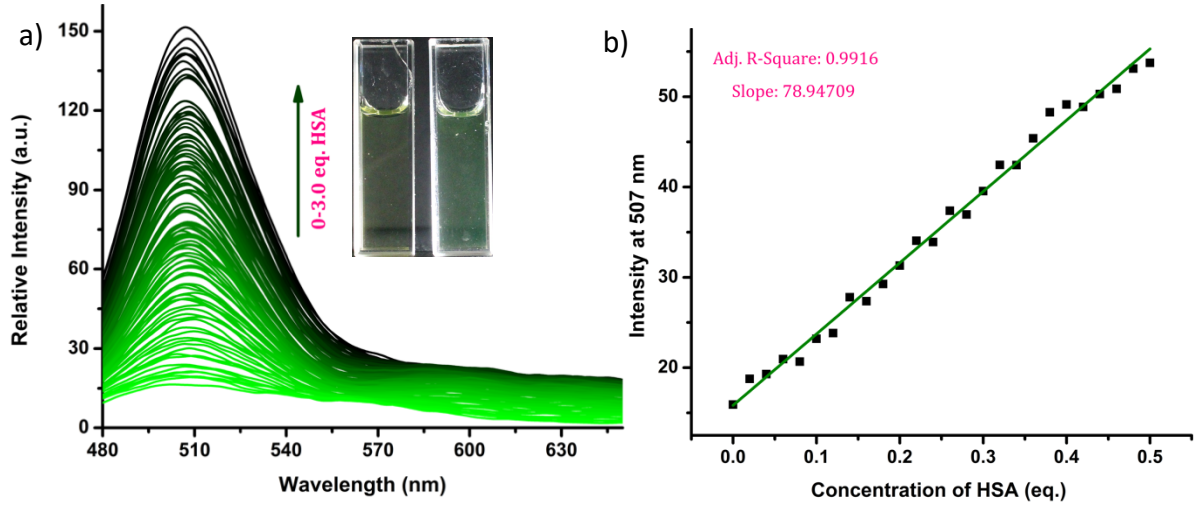

Figure S13. Fluorescence spectra of **2h** (1.66 μM) on incremental addition of HSA (0-3 eq.) in PBS buffer (pH 7.4, 1 mM) and photograph of **2h** in the absence and presence of HSA under flashlight (inset). b) Linear relationship between the concentration of HSA and fluorescence intensity of **2h** at 507 nm (λ_{ex}= 460 nm).

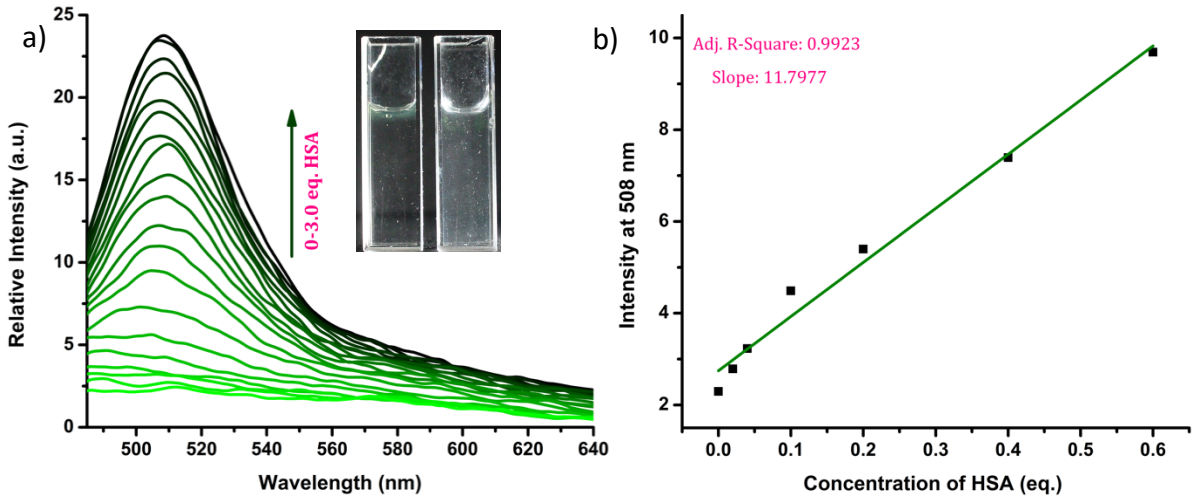

Figure S14. Fluorescence spectra of **2i** (1.66 µM) on incremental addition of HSA (0-3 eq.) in PBS buffer (pH 7.4, 1 mM) and photograph of **2i** in the absence and presence of HSA under flashlight (inset). b) Linear relationship between the concentration of HSA and fluorescence intensity of **2i** at 508 nm (λ_{ex}= 460 nm).

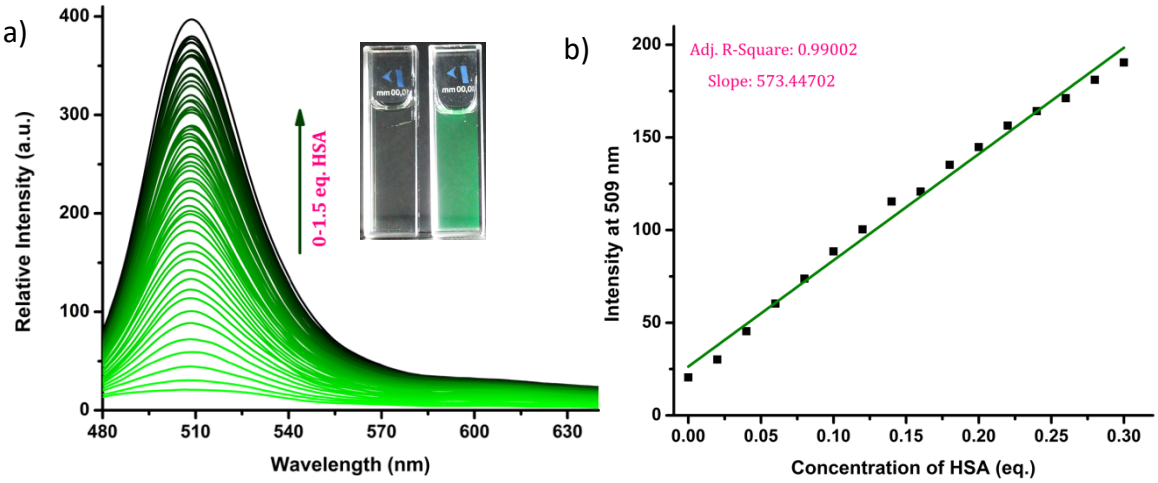

Figure S15. Fluorescence spectra of **2j** (1.66 µM) with incremental addition of HSA (0-1.5 eq.) in PBS buffer (pH 7.4, 1 mM) and photograph of **2j** in the absence and presence of HSA under flashlight (inset). b) Linear relationship between the concentration of HSA and fluorescence intensity of **2j** at 509 nm (λ_{ex}= 460 nm).

Table S2. Relative enhancement in emission intensity and LoD of **1d**, **2f**, **2g**, **2h**, **2i**, and **3d** in the presence of 1 eq. of HSA

Compound	Relative enhancement in emission intensity in the presence of 1 eq. of HSA	LoD (nM)
1d	1	-
2f	1.5	-
2g	1	-
2h	5	12.6
2i	2.5	63
3d	3	-

Response time

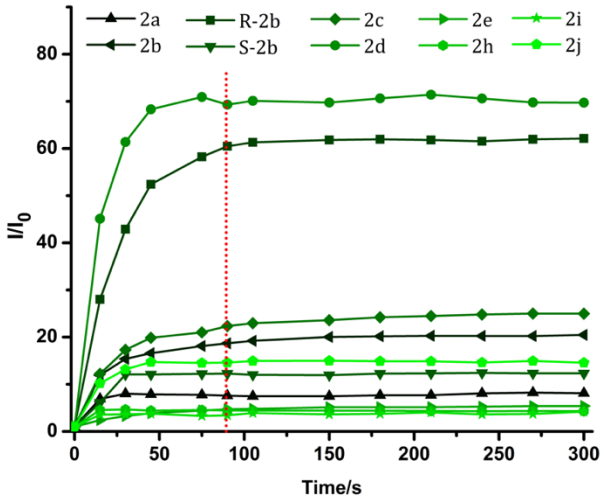

Figure S16. Time-dependent fluorescence response of 1.66 μM solution of **2a-e** and **2h-j** on the addition of HSA (1 eq.) in PBS buffer (pH 7.4, 1 mM); λ_{ex}= 460 nm.

Effect of pH

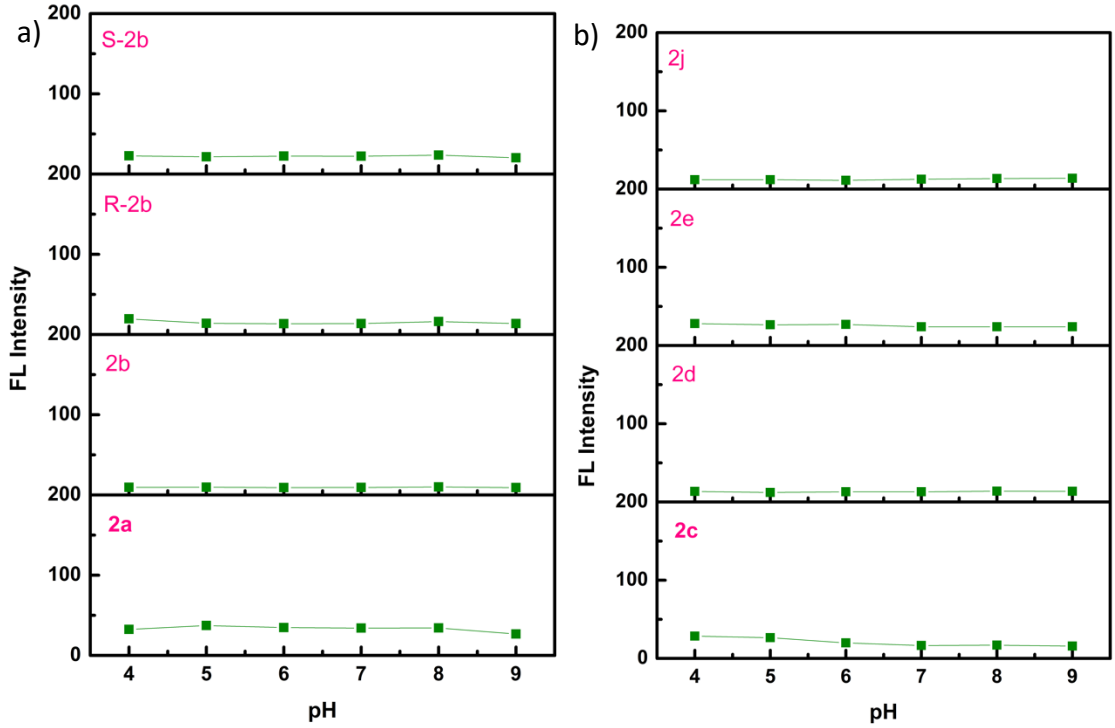

Figure S17. Fluorescence response of 1.66 μM solution of (a) **2a**, **2b**, **R-2b**, & **S-2b** and (b) **2c**, **2d**, **2e**, & **2j** at different pH in PBS buffer (1 mM); λ_{ex}= 460 nm.

Selectivity

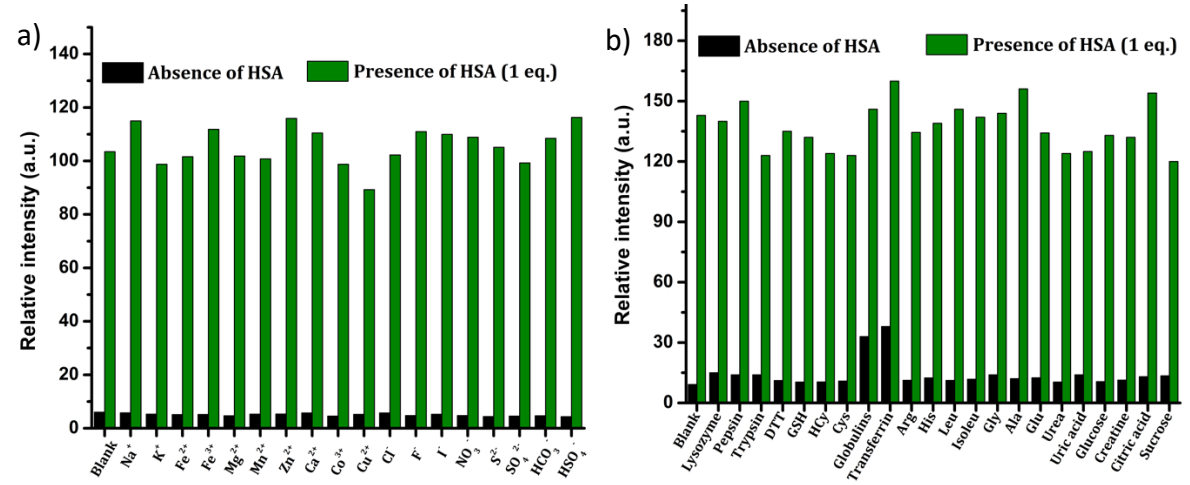

Figure S18. Fluorescence response of 1.66 μM solution of **2a** in PBS (pH 7.4, 1 mM) in the presence of various (a) metal ions & anions and b) proteins, thiols, amino acids, etc. 5 eq. of each of the interfering species were added; λ_{ex}= 460 nm.

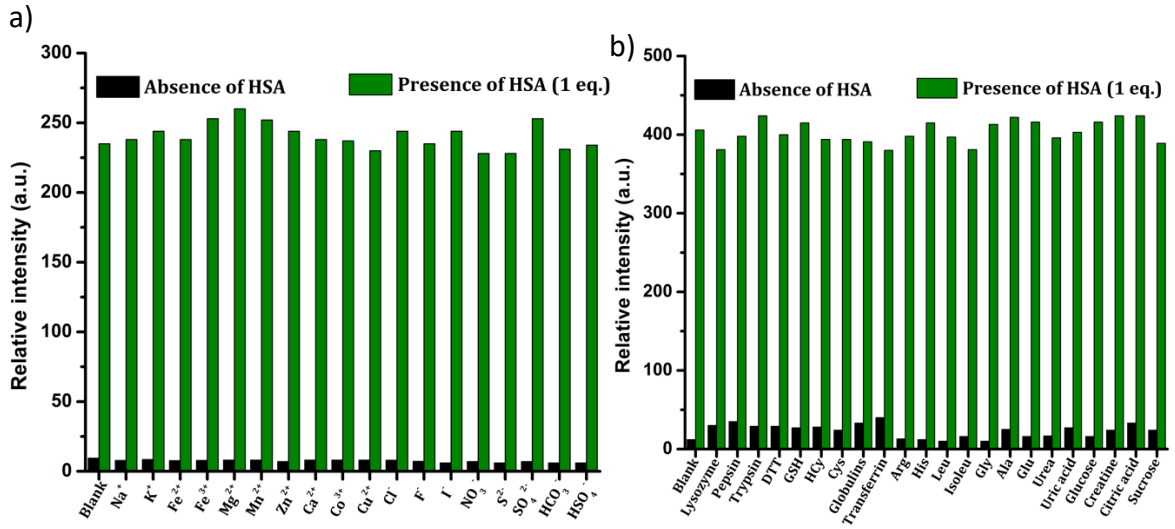

Figure S19. Fluorescence response of 1.66 µM solution of **2c** in PBS (pH 7.4, 1 mM) in the presence of various (a) metal ions & anions and b) proteins, thiols, amino acids, etc. 5 eq. of each of the interfering species were added; λ_{ex}= 460 nm.

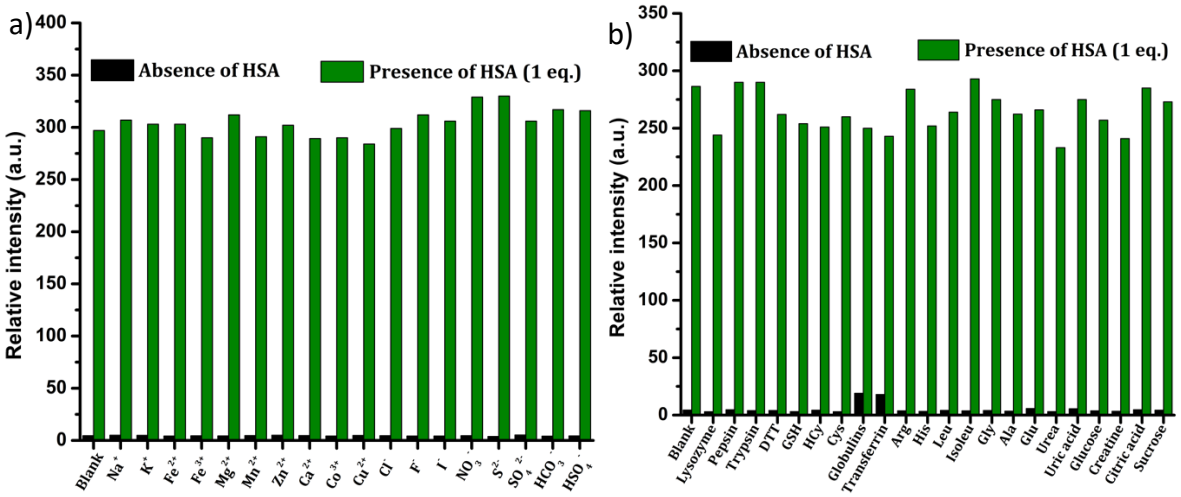

Figure S20. Fluorescence response of 1.66 µM solution of **2d** in PBS (pH 7.4, 1 mM) in the presence of various (a) metal ions & anions and b) proteins, thiols, amino acids, etc. 5 eq. of each of the interfering species were added; λ_{ex}= 460 nm.

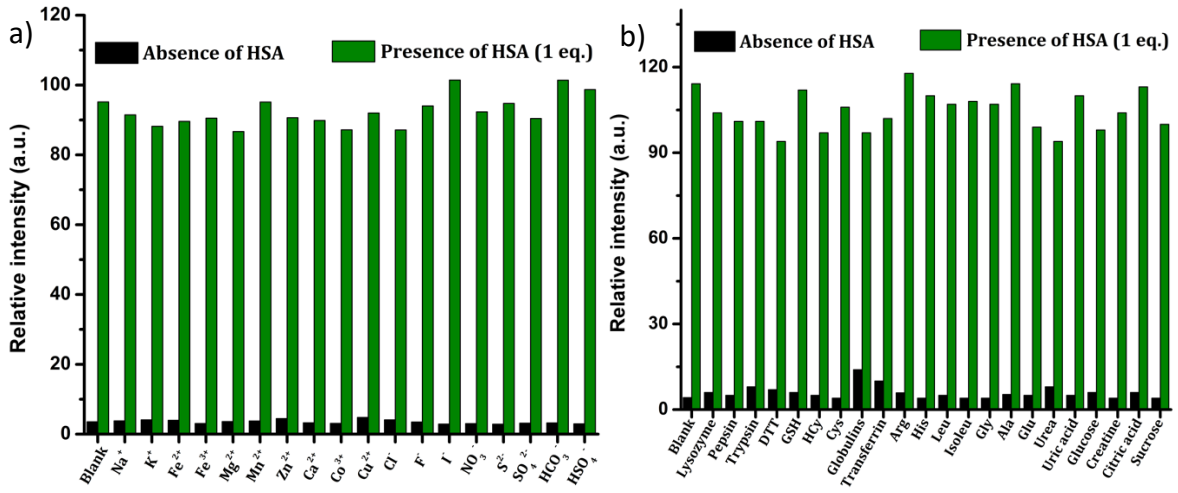

Figure S21. Fluorescence response of 1.66 μM solution of **2j** in PBS (pH 7.4, 1 mM) in the presence of various (a) metal ions & anions and b) proteins, thiols, amino acids, etc. 5 eq. of each of the interfering species were added; λ_{ex}= 460 nm.

Serum quantification

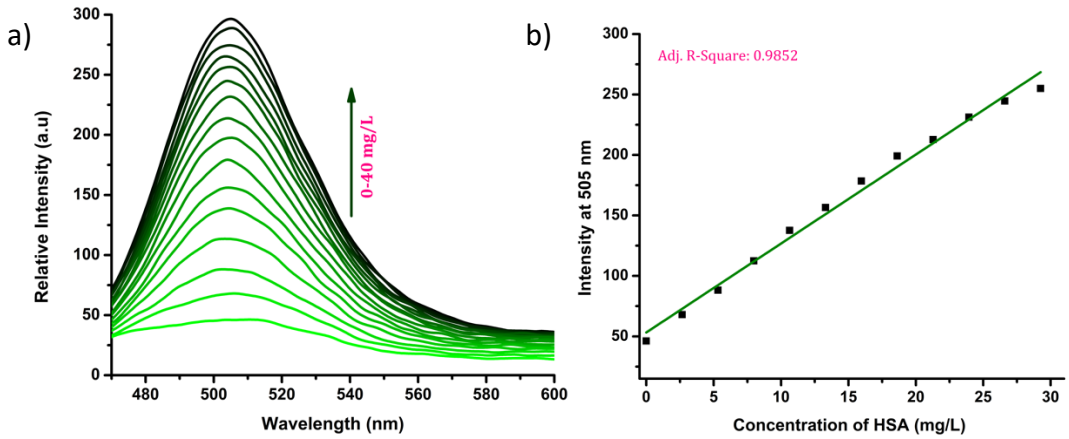

Figure S22. a) Emission spectra of **2d** (1.66 μM) in 3 mL PBS buffer (pH 7.4, 1 mM) on adding an increasing amount of standard serum (diluted 10 times, added 0-20 μL) and b) the corresponding calibration plot.

Urine quantification

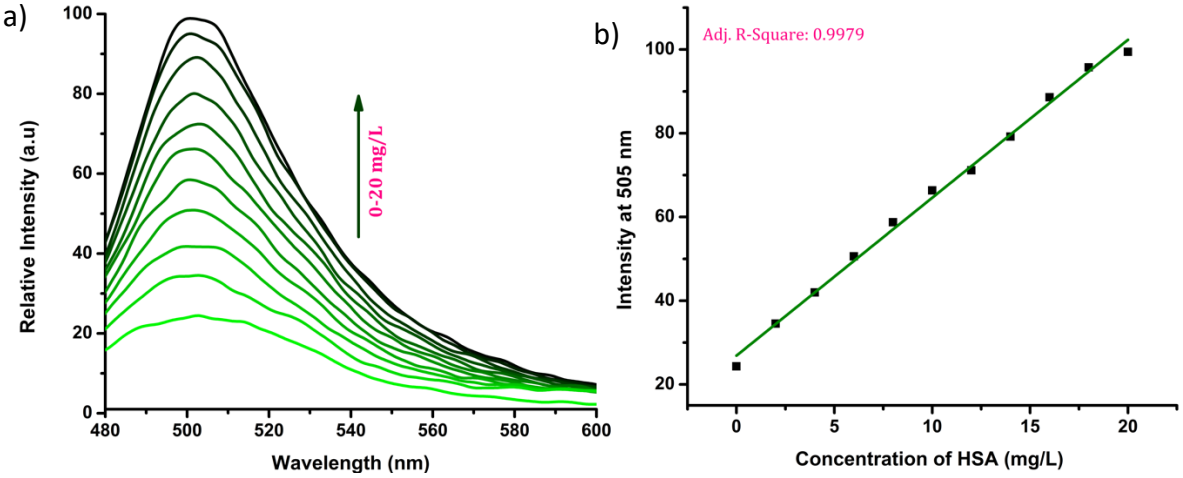

Figure S23. a) Emission spectra of **2d** (1.66 μM) in 3 mL PBS buffer (pH 7.4, 1 mM) on adding an increasing amount of urine (spiked with HSA) and b) the corresponding calibration plot.

Accuracy and recovery

Accuracy was determined by collecting data for three different serum samples (n=3) and the value is expressed as the percentage of recovery between the mean concentrations of HSA recovered and that of the original. The average recoveries and percentage relative error in measurements of three independent samples of **R-2b** are presented in Table S3.

Table S3. Determination of accuracy and percentage recovery.

Sample	**[HSA] as obtained using (g/dL)**		**% Average recovery (r)**	**% Relative error (δ)**
	BCG method	**R-2b (C_{HSA}) (Mean ± SD, n=3)**		
1	3.8	3.84±0.08	101.05	1.05
2	4.1	4.15±0.11	101.21	1.21
3	3.9	3.97±0.03	101.79	1.79
4	2	1.65±0.03	82.5	17.5
5	2.7	2.54±0.02	94.07	5.93

% Average recovery (r) = $100*C_{HSA}/ C_{BCG}$

% Relative error (δ) = $100*(C_{HSA} - C_{BCG})/ C_{BCG}$

Robustness

The robustness of the method was validated by performing the measurements at slightly different emission wavelengths. All parameters except the wavelength were made constant during the process. Seven independent measurements (n=7) of a selected serum sample were done at each of these wavelengths. The statistical comparison was done with Friedman analysis and no significant difference was found between the results (Table S4).

Table S4. Robustness data of the method.

[HSA] (g/dL) BCG method	**Wavelength (nm)**	**Found [HSA] (g/dL) (Mean ± SD, n=7)**	**% RSD**
3.8	**458**	3.77±0.03	0.79
	460	3.76±0.03	0.79
	462	3.78±0.02	0.52
	Friedman analysis: p= 0.0663 > p=0.05		

Precision

In order to find the precision of the method, three different serum samples were analyzed in three independent runs on the same day (intra-day precision). The precision of the analysis method was determined by calculating the relative standard deviation (RSD %). The RSD values obtained are presented in Table S5.

Table S5. Determination of intra-day precision.

[HSA] (g/dL) BCG method	**Found [HSA] (g/dL) (Mean ± SD, n=3)**	**% RSD**	**± SE**
3.8	3.86±0.06	1.55	0.03
4.1	4.06±0.12	2.95	0.06
3.9	3.85±0.04	1.03	0.02
2	1.75±0.02	1.14	0.01
2.7	2.52±0.03	1.19	0.01

Standard deviation (SD) = square root of $\Sigma(m\text{-}i)^2/n\text{-}1$ (m is the mean)

Percentage relative standard deviation (%RSD) = 100*(SD/m)

Standard error (SE) =SD/√n

Job's plot analysis

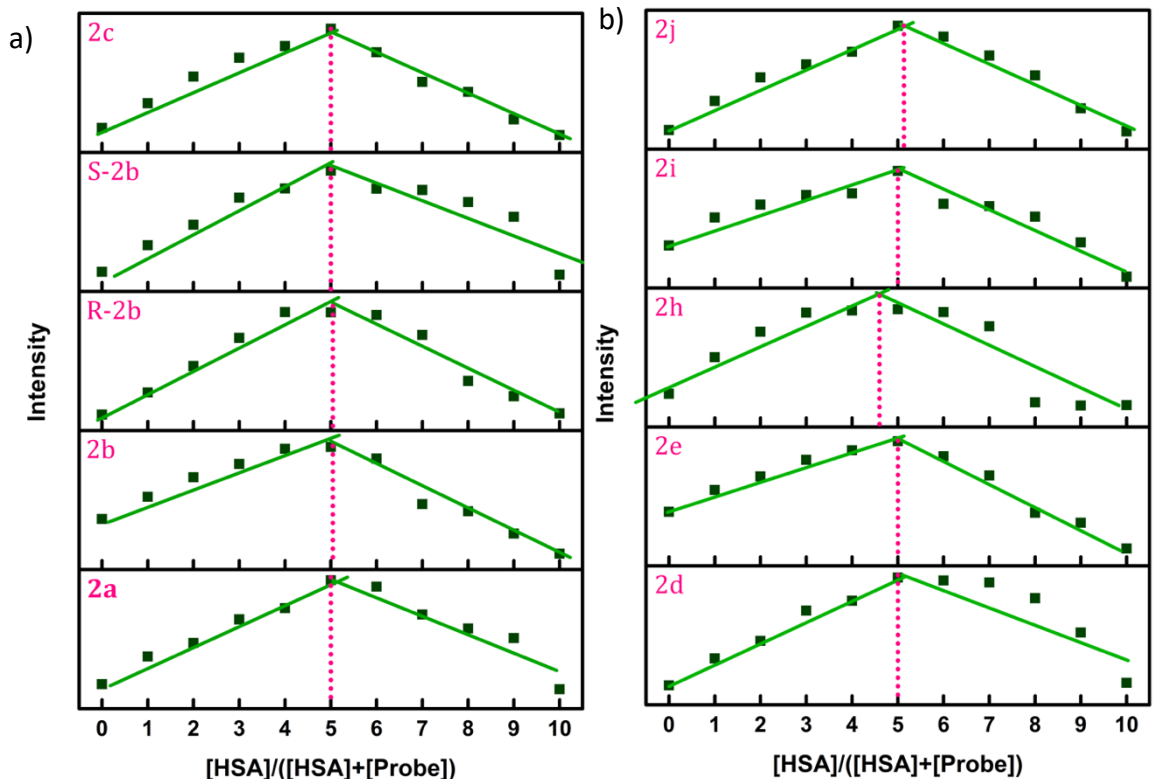

Figure S24. Job's plot of compounds with HSA at varying ratios of probe and HSA. Total concentration ([HSA]+[Probe]) maintained at 3.33 μM in PBS buffer (pH 7.4, 1 mM); λ_{ex}= 460 nm.

Effect of denaturation of HSA

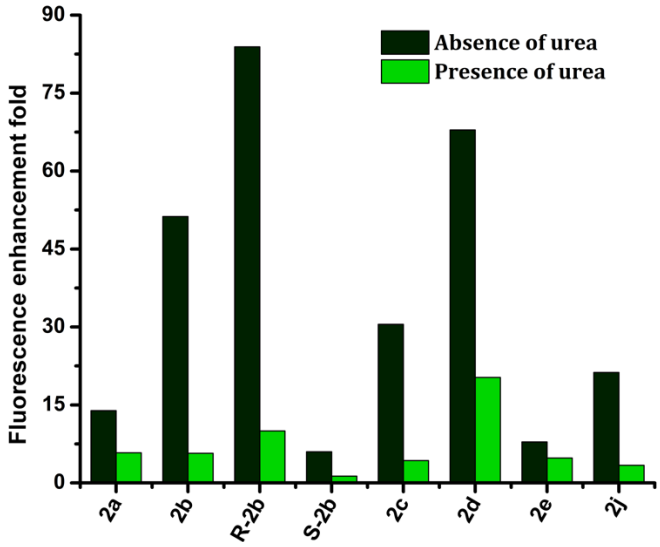

Figure S25. Enhancement in the fluorescent intensity of HSA complex of **2a-2e**, **R-2b**, **S-2b**, and **2j** in the absence and presence of 9 M urea in PBS buffer (pH 7.4, 1 mM); λ_{ex}= 460 nm.

Absorption spectra

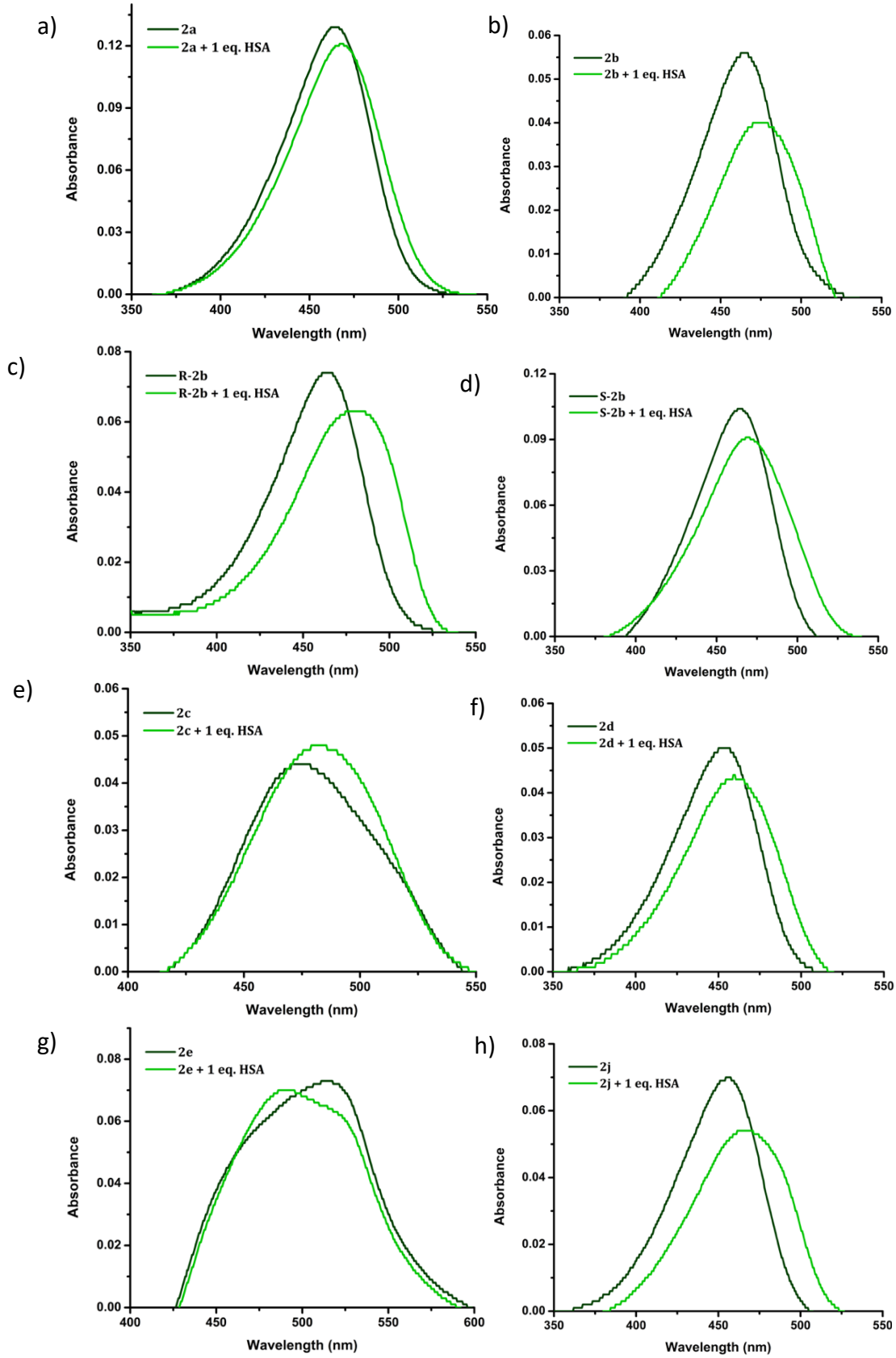

Figure S26. Absorption spectra of 1.66 μM solution of a) **2a**, b) **2b**, c) **R-2b**, d) **S-2b** e) **2c**, f) **2d**, g) **2e**, and h) **2j** in the absence and presence of HSA in PBS buffer (pH 7.4, 1 mM).

Site selectivity

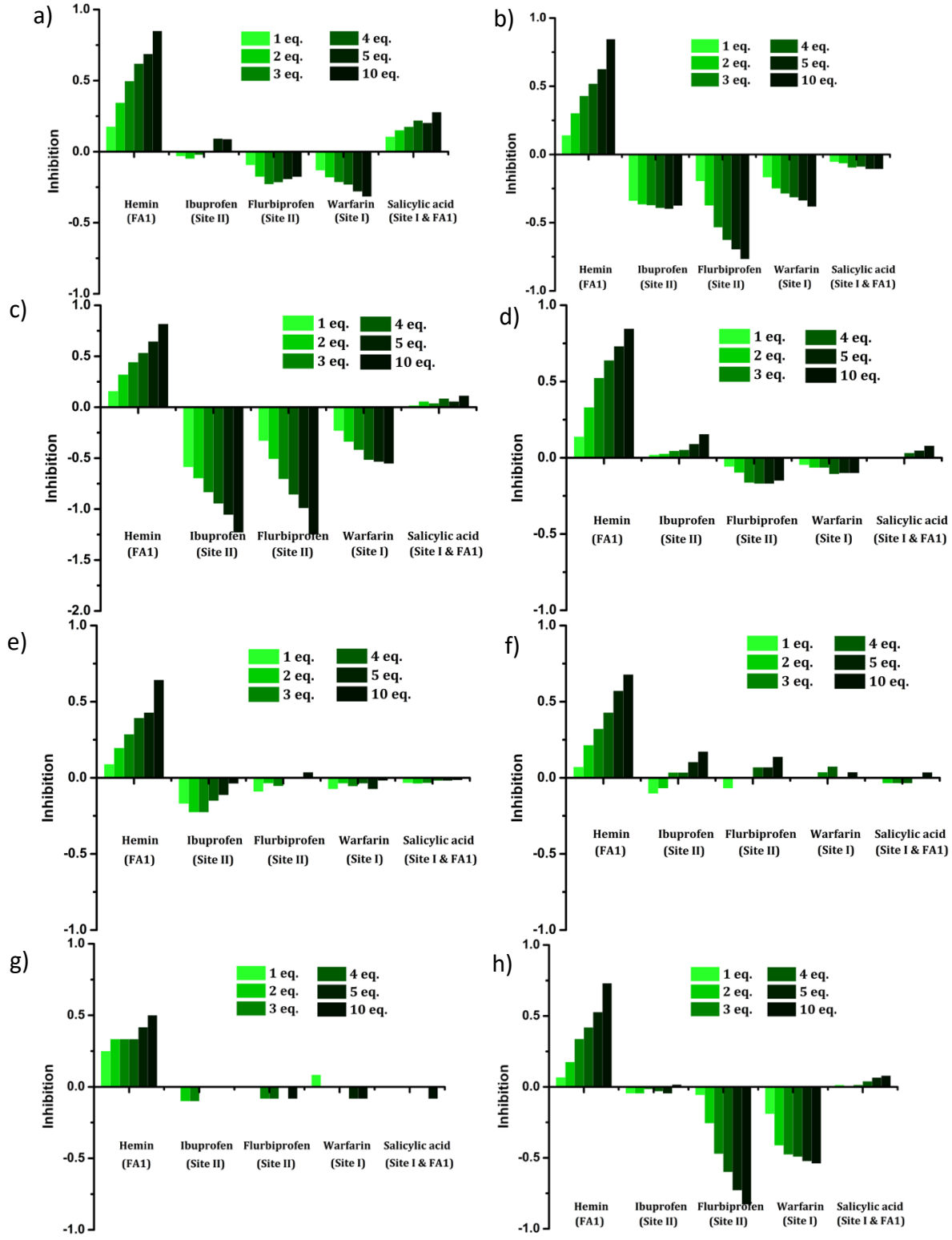

Figure S27. Inhibition of a) **2a**, b) **2b**, c) **R-2b**, d) **S-2b,** e) **2c**, f) **2e,** g) **2h**, h) **2i**, and i) **2j** binding in the presence of varying concentrations of site-specific markers. The composition of the complex is 1:1 (probe: HSA).

Docking studies

Table S6. Docking result of various ligands on FA1 binding site of HSA

No	Ligand	Binding Energy	Ligand Efficiency	Inhibition Constant
1	**2a**	-12.75	-0.42	453.7 pM
2	**S-2b**	-12.20	-0.39	1.14 nM
3	**R-2b**	-12.36	-0.40	876.2 pM
6	**2c**	-13.81	-0.41	74.94 pM
4	**2d**	-10.91	-0.04	9.98 nM
7	**2e**	-12.10	-0.37	1.34 nM
10	**2j**	-11.77	-0.41	2.35 nM

Table S7. Interactions of R-2b

Hydrophobic Interactions ····

Index	Residue	AA	Distance	Ligand Atom	Protein Atom
1	115A	LEU	3.09	20	1139
2	134A	PHE	3.73	29	1323
3	138A	TYR	3.02	20	1368
4	138A	TYR	3.44	27	1365
5	142A	ILE	3.32	13	1415
6	161A	TYR	3.98	22	1627
7	161A	TYR	3.80	28	1622
8	165A	PHE	3.20	29	1666
9	182A	LEU	3.60	22	1809
10	186A	ARG	3.38	14	1847
11	186A	ARG	3.28	15	1846
12	190A	LYS	3.22	14	1888

Hydrogen Bonds

Index	Residue	AA	Distance H-A	Distance D-A	Donor Angle	Protein donor?	Side chain	Donor Atom	Acceptor Atom
1	161A	TYR	2.07	2.96	156.18	✔	✔	1629 [O3]	3 [N1]
2	193A	SER	3.59	4.06	113.09	✔	✔	1915 [O3]	1 [N1]

π-Stacking

Index	Residue	AA	Distance	Angle	Offset	Stacking Type	Ligand Atoms
1	138A	TYR	4.07	16.01	1.50	P	25, 26, 27, 28, 29, 30
2	161A	TYR	4.02	10.68	1.78	P	25, 26, 27, 28, 29, 30

Table S8. Interactions of 2d

Hydrophobic Interactions

Index	Residue	AA	Distance	Ligand Atom	Protein Atom
1	115A	LEU	3.86	9	1135
2	135A	LEU	3.35	22	1330
3	138A	TYR	3.60	7	1368
4	138A	TYR	3.36	15	1366
5	139A	LEU	3.64	24	1377
6	142A	ILE	3.87	20	1411
7	161A	TYR	3.04	17	1625
8	161A	TYR	3.04	20	1624
9	161A	TYR	3.59	18	1623
10	161A	TYR	3.93	22	1620
11	182A	LEU	3.45	14	1809

Hydrogen Bonds

Index	Residue	AA	Distance H-A	Distance D-A	Donor Angle	Protein donor?	Side chain	Donor Atom	Acceptor Atom
1	117A	ARG	2.49	2.89	102.58	✔	✖	1148 [Nam]	1 [N1]

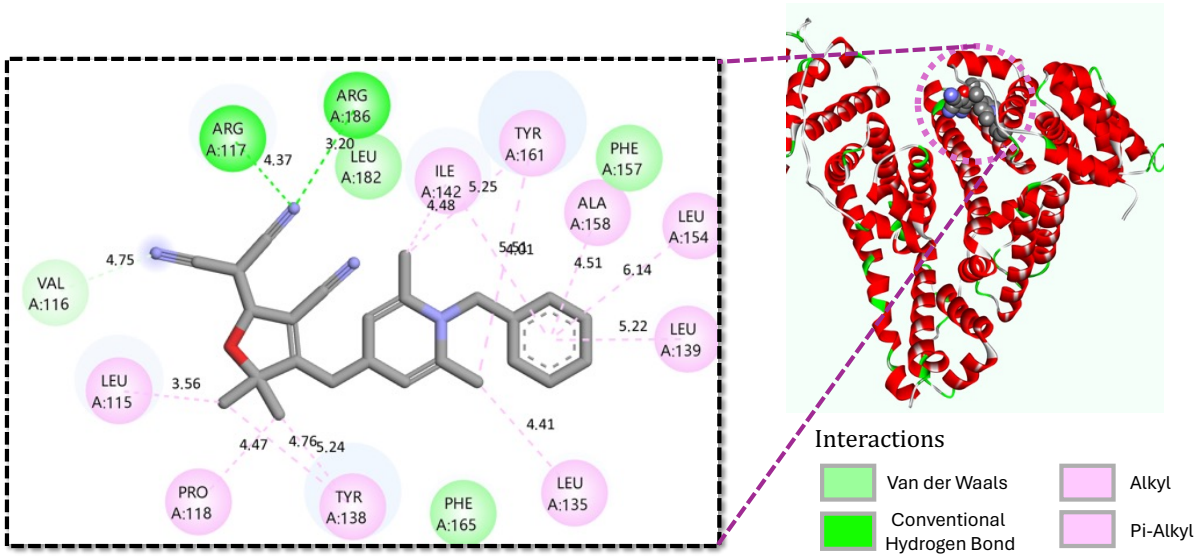

Figure S28. Molecular docking for the binding of **2a** at FA1 binding site of HSA and the predicted interactions with the surrounding amino acid residues.

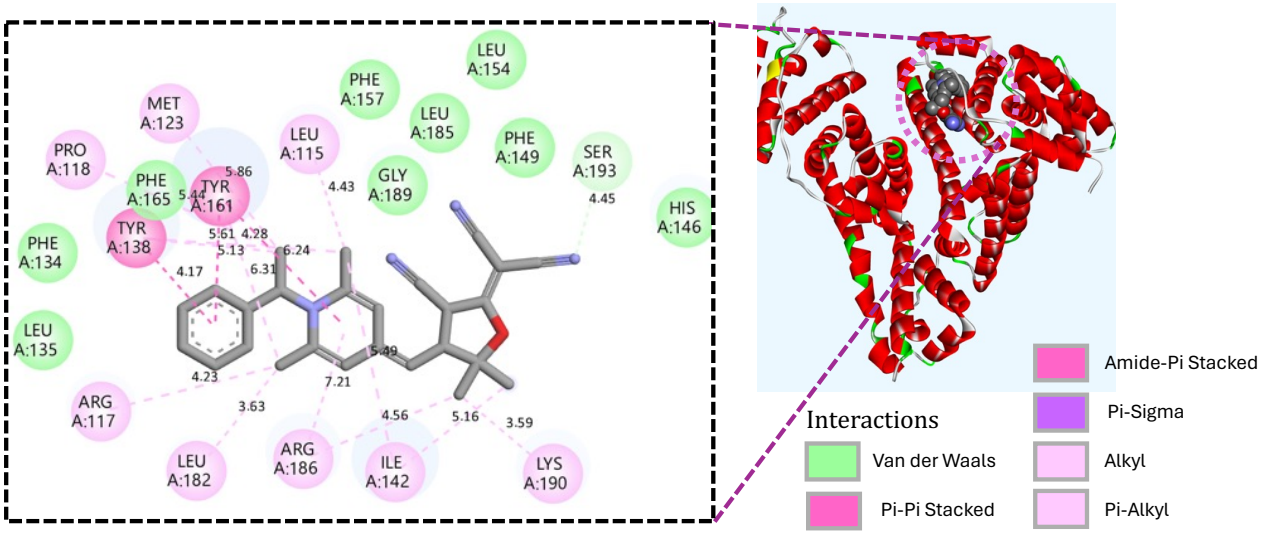

Figure S29. Molecular docking for the binding of **R-2b** at FA1 binding site of HSA and the predicted interactions with the surrounding amino acid residues.

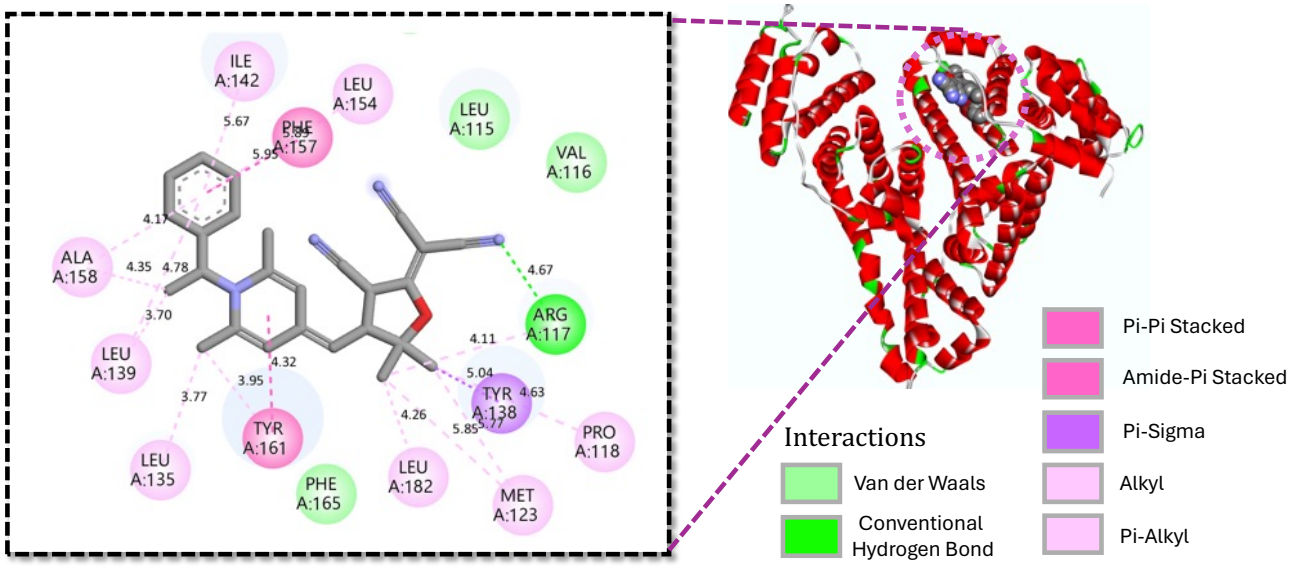

Figure S30. Molecular docking for the binding of **S-2b** at FA1 binding site of HSA and the predicted interactions with the surrounding amino acid residues.

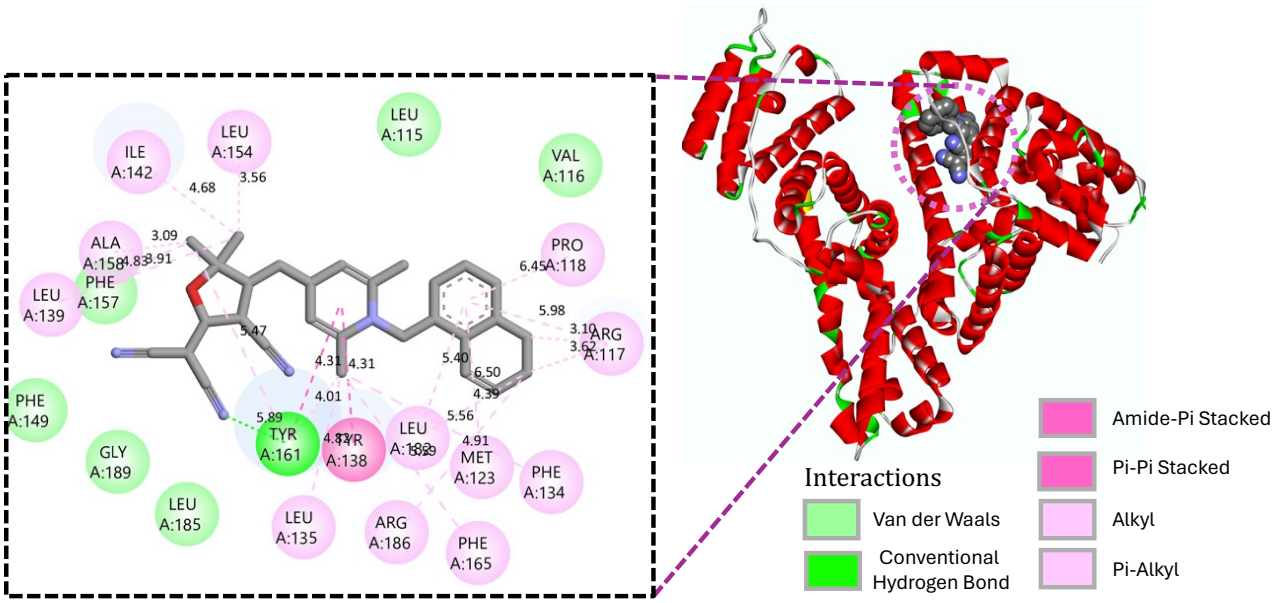

Figure S31. Molecular docking for the binding of **2c** at FA1 binding site of HSA and the predicted interactions with the surrounding amino acid residues.

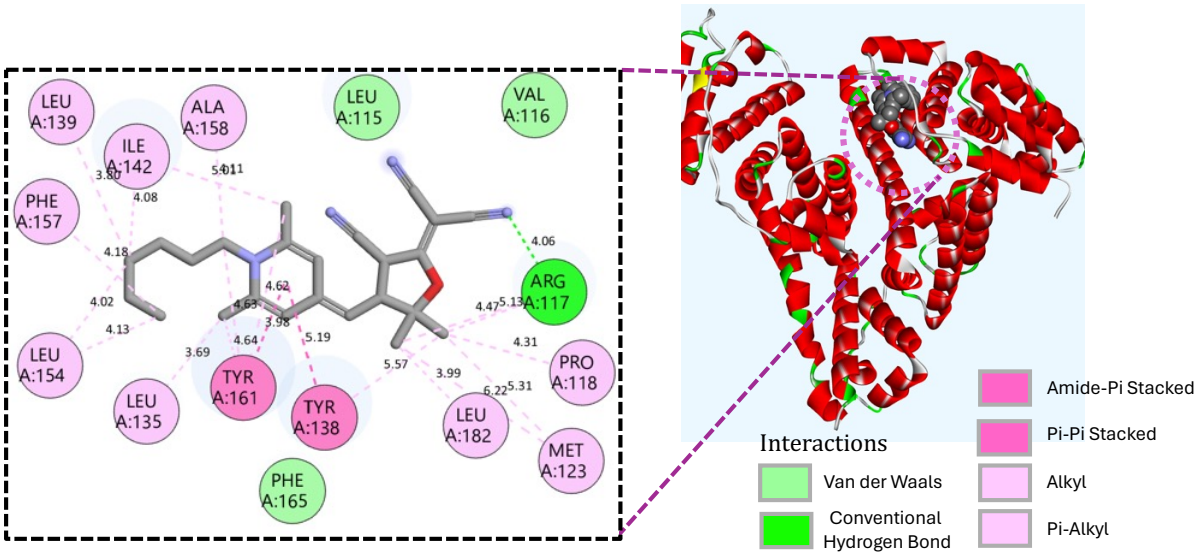

Figure S32. Molecular docking for the binding of **2d** at FA1 binding site of HSA and the predicted interactions with the surrounding amino acid residues.

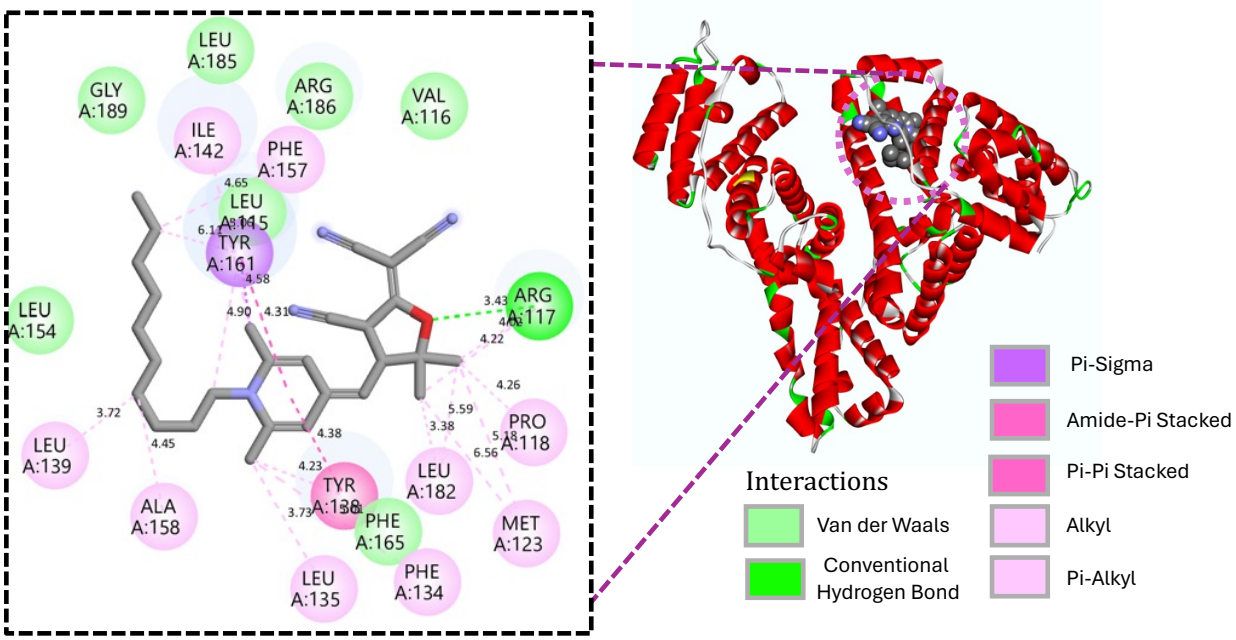

Figure S33. Molecular docking for the binding of **2e** at FA1 binding site of HSA and the predicted interactions with surrounding amino acid residues.

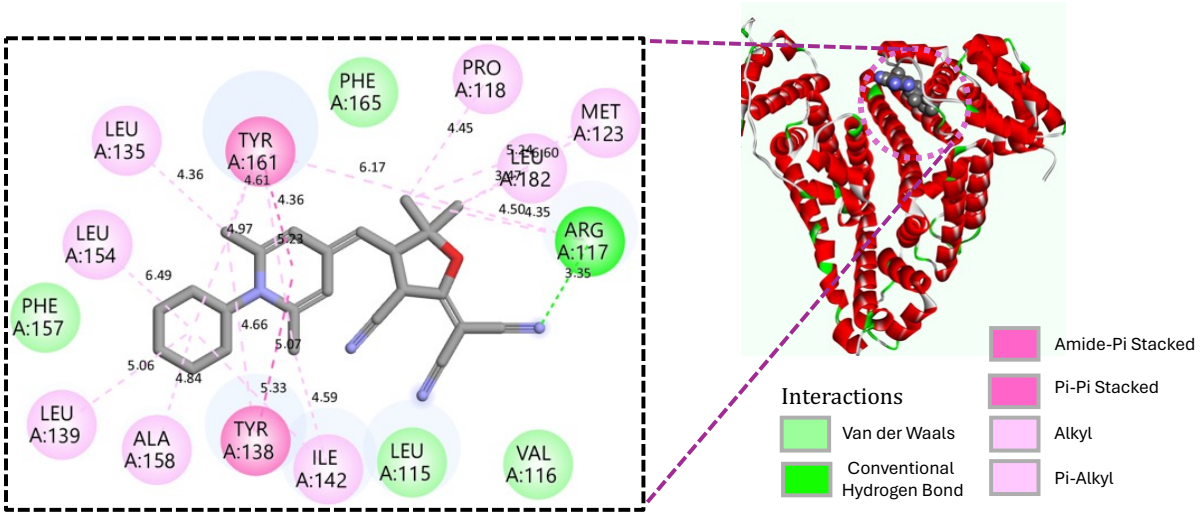

Figure S34. Molecular docking for the binding of **2j** at FA1 binding site of HSA and the predicted interactions with surrounding amino acid residues.

Reference

(1) Kanneth, S. S.; Mathew, D.; Parameswaran, P.; Sajeev, A. K.; Unni, K. N. N.; Chakkumkumarath, L. Substituent-Controlled Photophysical Responses in Dihydropyridine Derivatives and Their Application in the Detection of Volatile Organic Contaminants. *J. Org. Chem.* **2023**, *88* (21), 15007–15017. https://doi.org/10.1021/acs.joc.3c01455.